Challenges in Radiative Transfer Modeling Related to Advanced Data Assimilation

Dr. Fuzhong Weng

NOAA Center for Satellite Applications and Research
and
Joint Center for Satellite Data Assimilation

CRTM Software Architecture, Sciences and Physical Processes

- Atmospheric gaseous absorption
  - Band absorption coeff trained by LBL spectroscopy data with sensor response functions
  - Variable gases (H2O, CO2, O3 etc) .
  - Zeeman splitting effects near 60 GHz
- Cloud/precipitation scattering and emission
  - Fast LUT optical models at all phases including non-spherical ice particles
  - Gamma size distributions
- Aerosol scattering and emission
  - GOCART 5 species (dust, sea salt, organic/black carbon,)
  - Lognormal distributions with 35 bins
- Surface emissivity/reflectivity
  - Two-scale microwave ocean emissivity
  - Large scale wave IR ocean emissivity
  - Land mw emissivity including vegetation and snow
  - Land IR emissivity data base
- Radiative transfer scheme
  - Tangent linear and adjoints
  - Inputs and outputs at pressure level coordinate
  - Advanced double and adding scheme
  - Other transfer schemes such as SOI, Delta Eddington

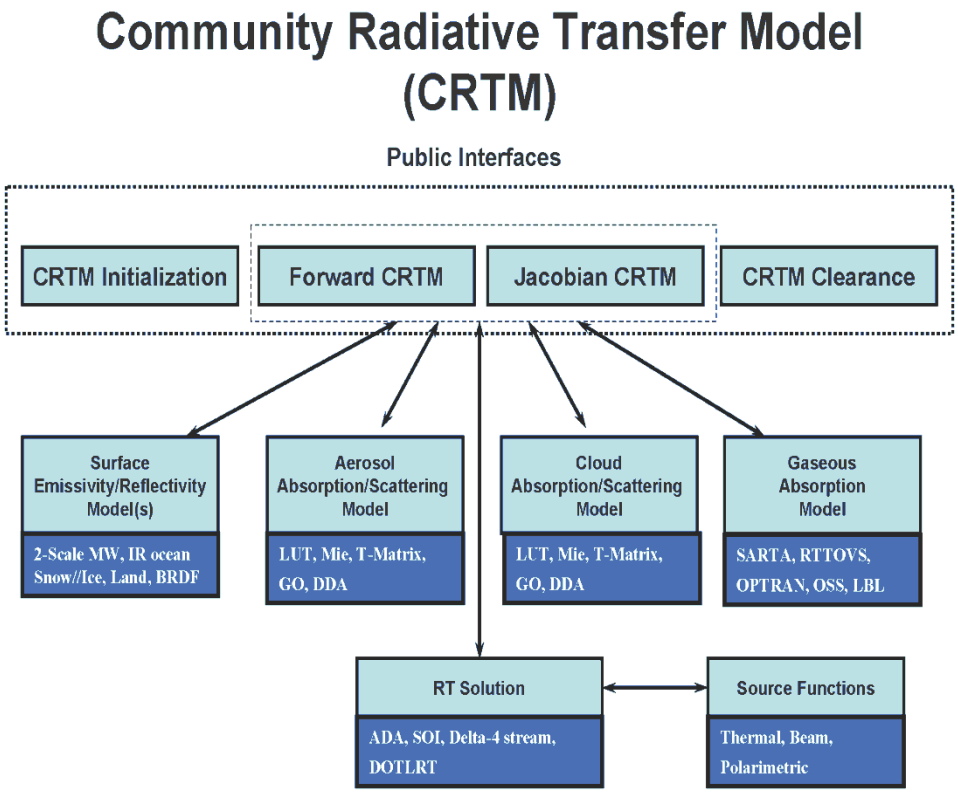

"Technology transfer made possible by CRTM is a shining example for collaboration among the JCSDA Partners and other organizations, and has been instrumental in the JCSDA success in accelerating uses of new satellite data in operations" – Dr. Louis Uccellini, Director of National Centers for Environmental Prediction

Major Applications of CRTM at NESDIS/STAR

- GOES-R and JPSS space sensor simulations and proxy data
- GOES-R Algorithm Working Group (L2 Products)
- NOAA/METOP, SNPP and JPSS instrument calibration
- Microwave Integrated Retrieval System (MIRS)
- Satellite radiance reprocessing for climate data records
- OSE on impacts of new satellite data in HWRF/GSI

Investigations of CRTM Modules and Their Performance

- Cloud scattering and absorption table at infrared wavelengths
- Comparison of Mie LUT with discrete dipole approximation (DDA) at microwave frequencies
- Validation of CRTM cloudy radiances using CloudSat data
- NLTE and solar reflection modules at CrIS SW
- Azimuthal dependence of microwave imager and sounder radiance simulation

Comparison of Cloud Scattering and Absorption Between CRTM and RTTOV

	CRTM	**RTTOV (RTTOV-SCATT)**
Radiative Transfer Solver	Advanced Adding and Doubling (ADA) scheme	Delta-Eddington Approximation
Scattering Properties (look-up table approach)	Precalculated using Mie theory and tabulated as a function of frequency, temperature, **radii**, and hydrometeor type and density	Precalculated using Mie theory and tabulated as a function of frequency, temperature, and hydrometeor type and density. DDA
Cloud types	Water, ice, rain, snow, graupel and hail	Water, ice, rain, and snow
Cloud cover	Not handle yet	Cloud fraction profile

Cloud Absorption and Scattering

In current CRTM:

- Six Cloud Types
  water, ice, rain, snow, graupel, and hail

- NESDIS Look-up Table
  mass extinction coefficient, single scattering albedo, asymmetric factor and Legendre phase coefficients

  Sources:
  IR: 1) Spherical water cloud droplets (Simmer, 1994)
  Non-spherical ice cloud particles (Yang et al., 2005)
  2) Mie scattering with modified gamma size distributions

  MW: 1) Spherical cloud, rain and ice particles (Simmer, 1994)
  2) Mie scattering with modified gamma size distribution

Cloud Absorption/Scattering Module

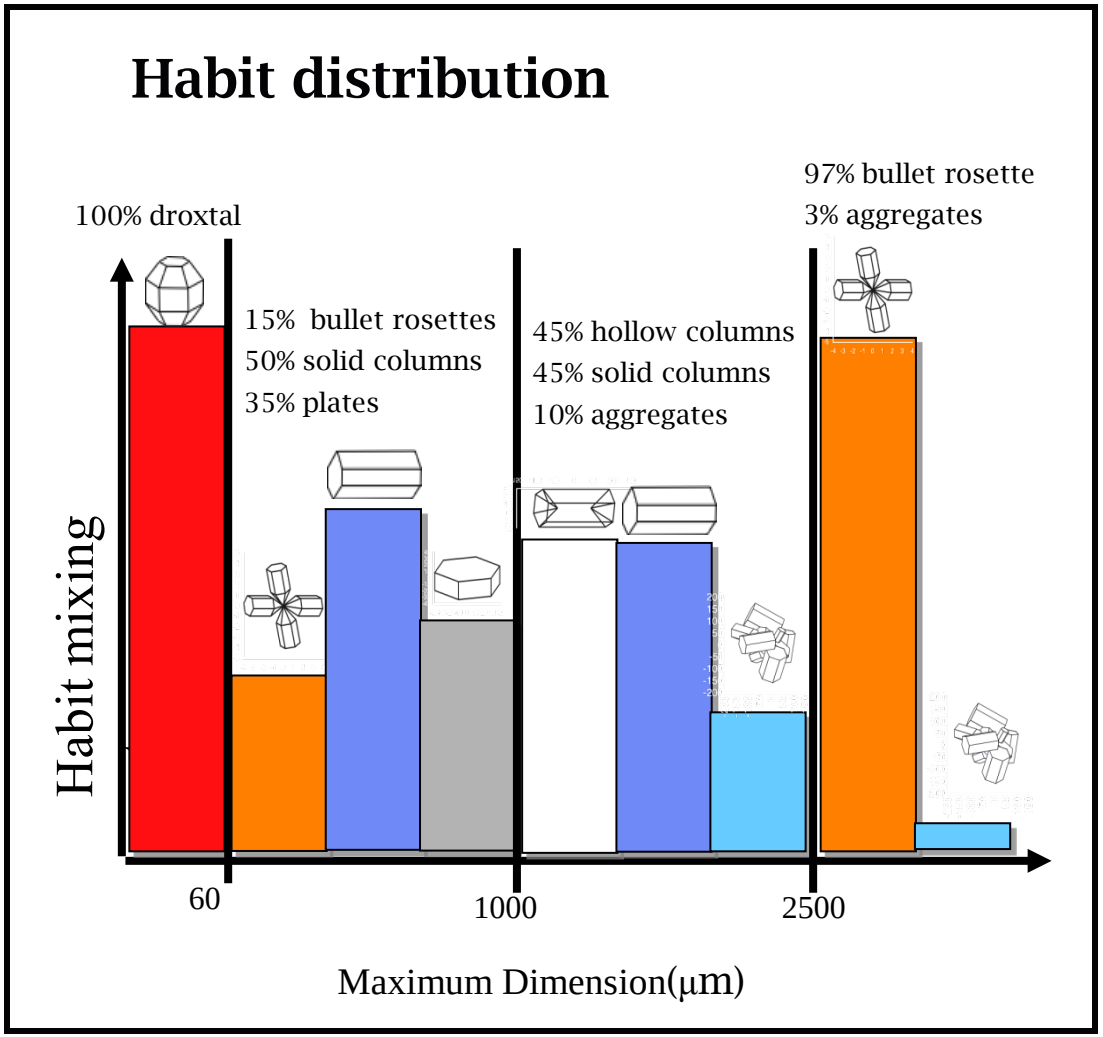

Cloud Types:

water ice
rain snow
graupel hail

Look-up Table:

mass extinction coefficient
single scattering albedo
Asymmetric factor
Legendre phase coefficients

✓ spherical cloud droplets (Simmer, 1994)

✓ non-spherical ice cloud particles (Yang et al., 1997; Macke, Mishenko et al.; Baum et al., 2001)

Observed and CRTM Simulated SEVIRI Channel 3

SEVIRI Observation

Simulated with ECMWF Cloud

Simulated with IR Cloud

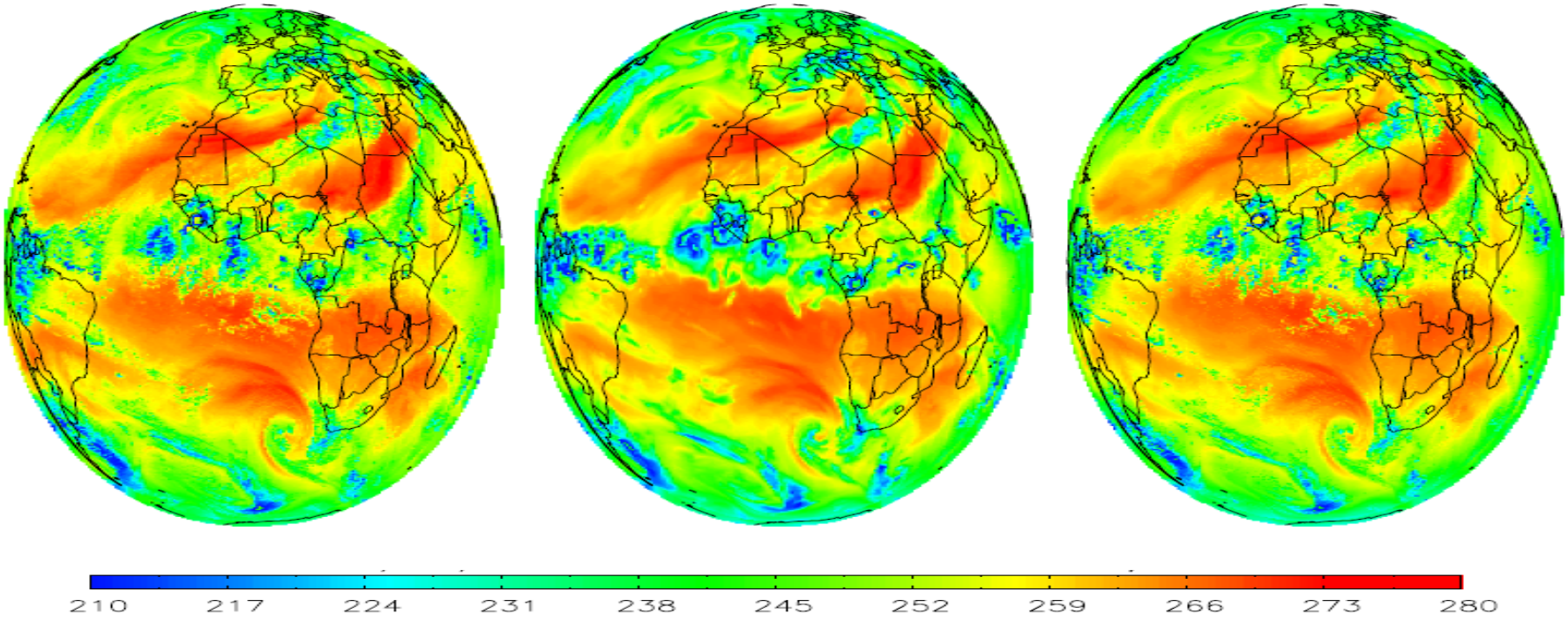

0030 Z May 20, 2008, 7.35μm

Observed and CRTM Simulated SEVIRI Channel 4

SEVIRI Observation

Simulated with ECMWF Cloud

Simulated with IR Cloud

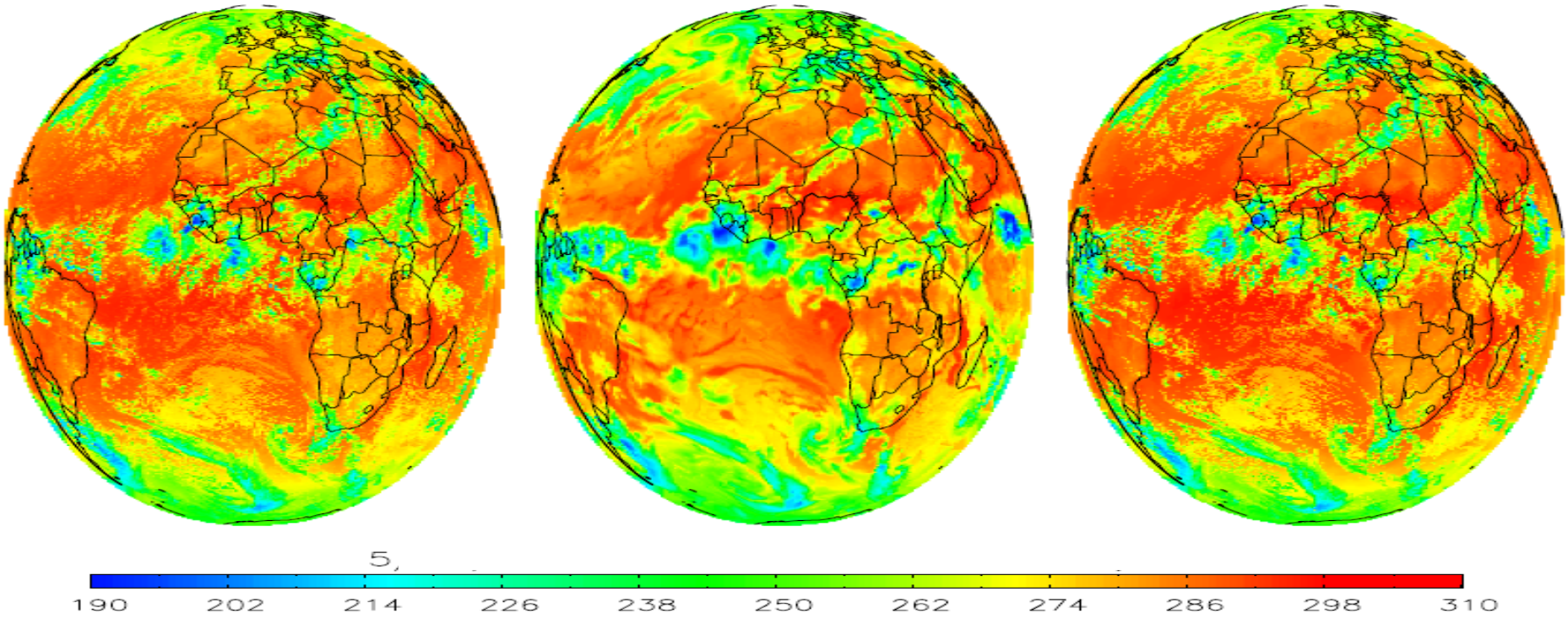

0030 Z May 20, 2008, 8.7µm

SEVIRI Observations vs Simulations

Channel	Clear-Sky		ECMWF		ECMWF+IR Cloud	
	Bias	Sigma	Bias	Sigma	Bias	Sigma
1	-30.14	36.39	-4.06	15.90	-1.29	2.02
2	-4.39	8.71	-0.02	6.33	-0.79	2.20
3	-12.46	18.35	-0.72	10.80	-0.83	1.86
4	-34.12	40.41	-2.46	17.05	-0.11	1.38
5	-19.10	23.73	-2.19	9.73	-0.44	1.46
6	-36.02	42.64	-1.82	17.97	0.48	1.48
7	-35.18	41.73	-1.80	17.82	0.36	1.47
8	-20.97	26.85	-0.93	12.54	-0.40	1.56

CIMSS RTM and CRTM

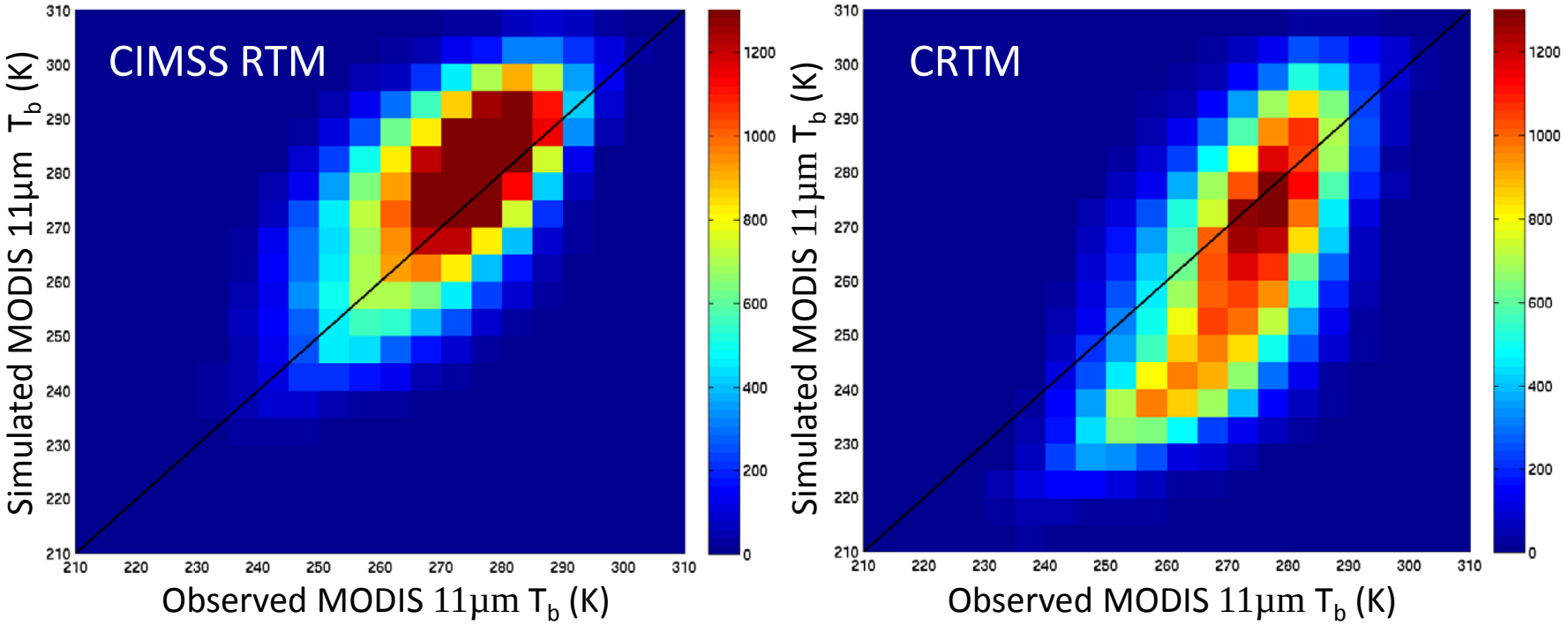

- Single layer ice clouds ($\tau < 6$) as identified by CloudSat for 2007
- **RTM input:** ECMWF temp/humid profiles; collocated CloudSat IWC profiles and MODIS cloud effective radius retrievals

Effects of Precipitating Clouds on AMSU

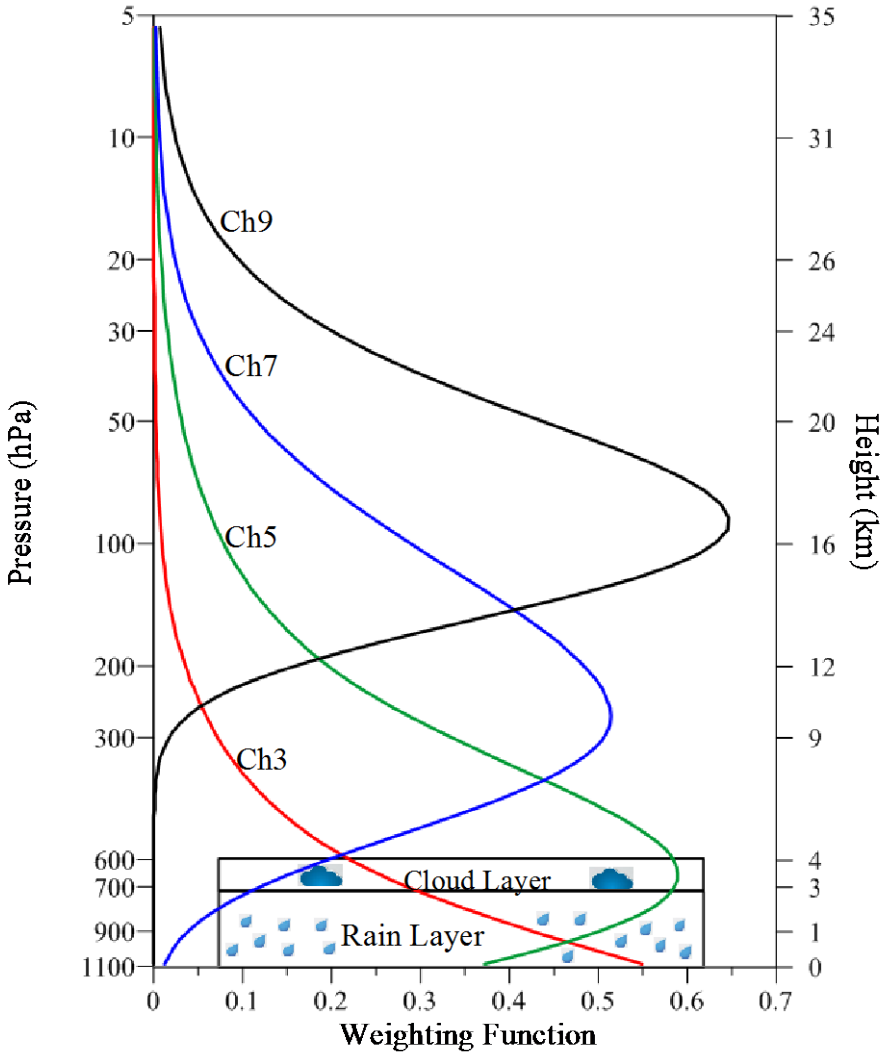

Effects of Precipitating Clouds on AMSU TB

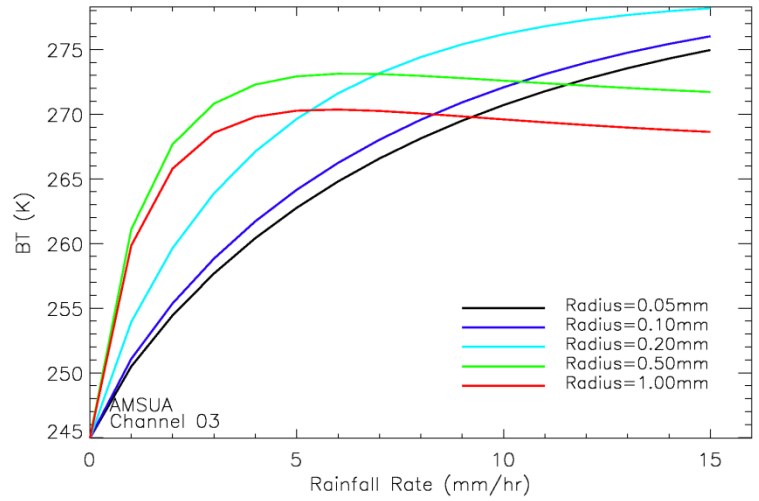

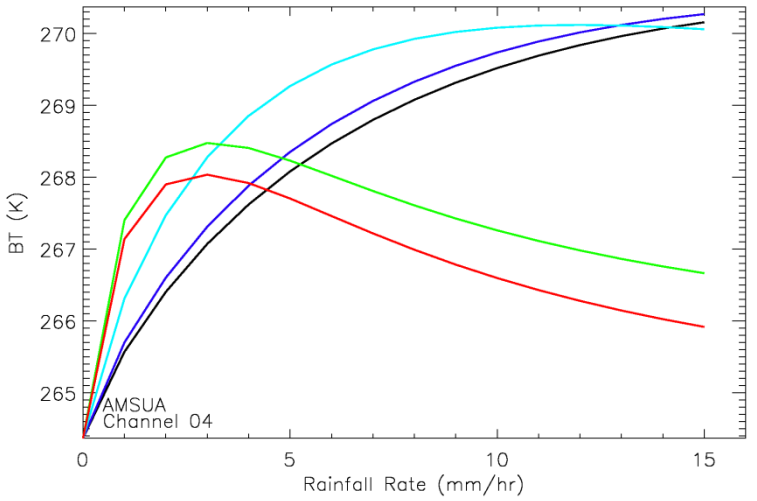

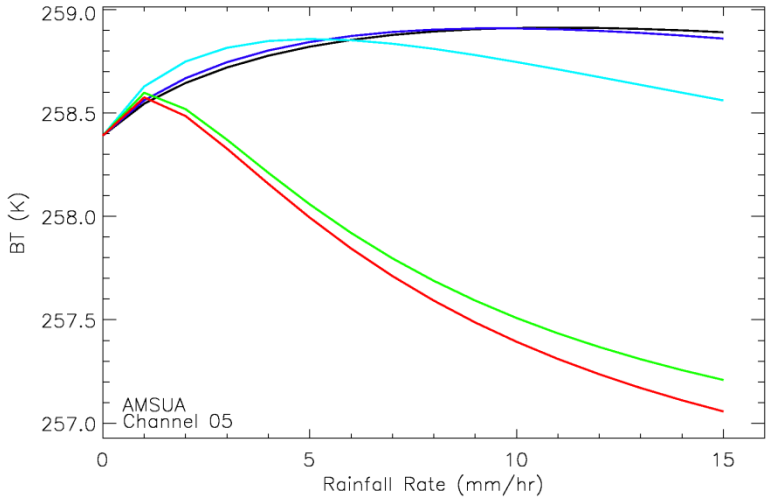

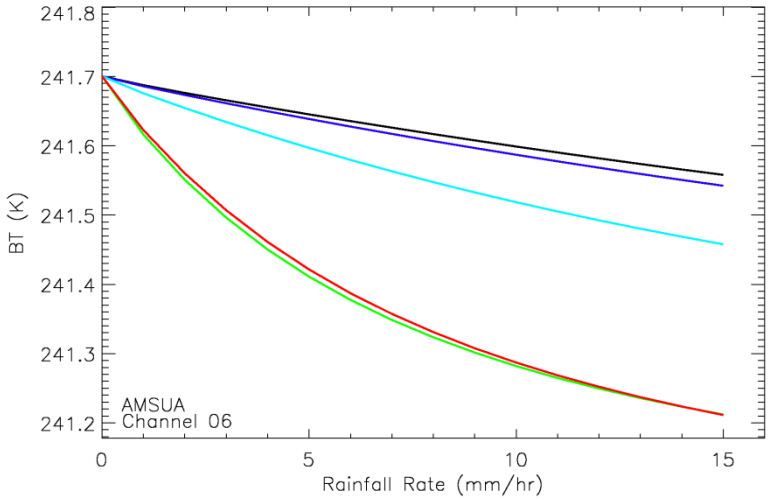

Assume a stratiform rainfall with intermediate rainfall rate: A cloud layer about 0.8 km depth below the freezing level with liquid water path of 0.5 kg/m2, and the raindrops all below the non-precipitating cloud layer and the rainfall rates unchanged vertically. Emissivity set to 0.5.

Comparison Between CRTM and RTTOV in Liquid-Phase Cloud Conditions over Oceans

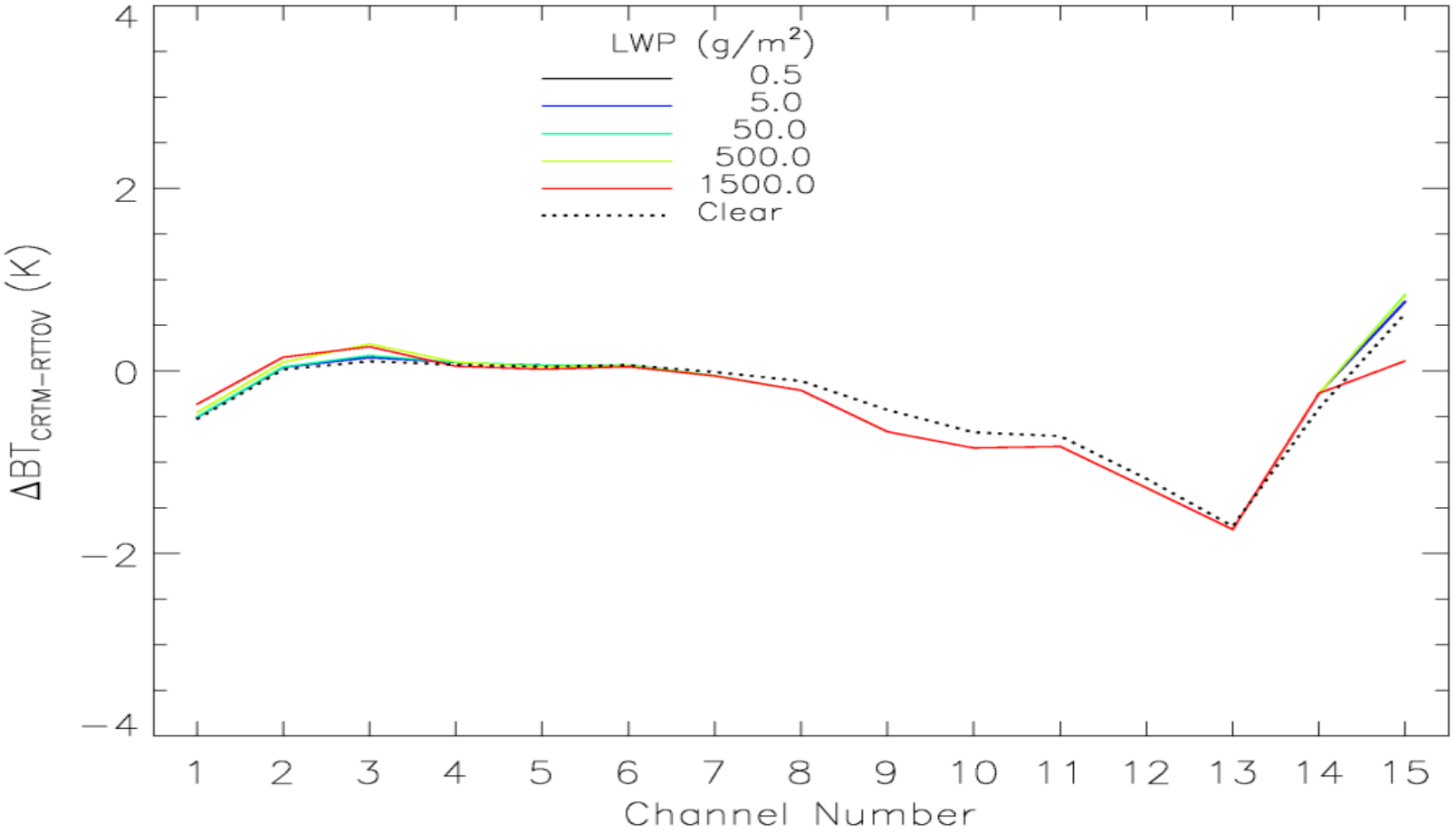

- A water cloud is placed at between 3.23 km-4.34 km.
- RTTOV-SCATT has N=60 model layers between surface and 0.1 hPa, and RTTOV coefficient has 43 layers. Interpolation is needed even for the same profile.
- The larger difference between CRTM and RTTOV for upper levels (for channels 9-13) most come from temperature interpolation errors.

Comparison Between CRTM and RTTOV in Precipitation Conditions

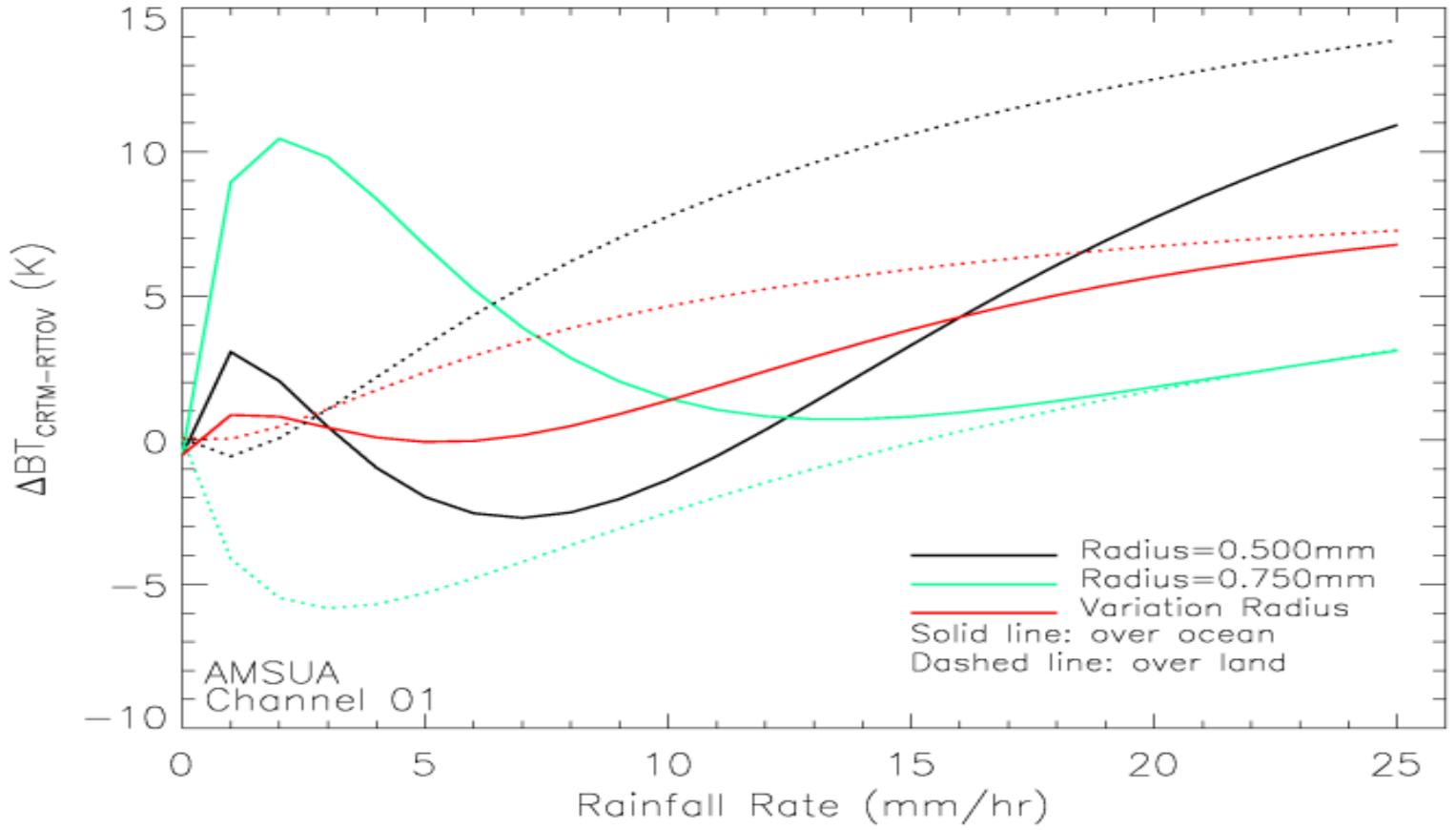

- Stratiform rainfall with intermediate rainfall rate. Thin ice layer topped rain cloud with constant rainfall rates below 4 km.
- BTs have high sensitivity to mean rain particle size.

Validation of CRTM Cloudy Radiances

- **CloudSat data**

  Afternoon satellite, Local time ascending node 1:31pm

  – Cloud Geometrical Profile: 2B-GEOPROF
  – Cloud Classification: 2B-CLDCLASS
  – Cloud Liquid/ICE Water Content & particle size: 2B-CWC-RO

- **Analyses**

  Temperature, water vapor and O_3 profiles and surface state

  – ECMWF analysis data set: ECMWF-AUX
  –NCEP surface analysis data set

- **NOAA 18 data**

  Afternoon satellite, Local time ascending node 1:38pm

  –AMSUA Level 1B and Level 2 data set
  – MHS Level 1B and Level 2 data set
  – AVHRR/3 Level 1B (GAC) data set

CRTM Validation Using CloudSat Data

NOAA 18 Orbit Data Matching

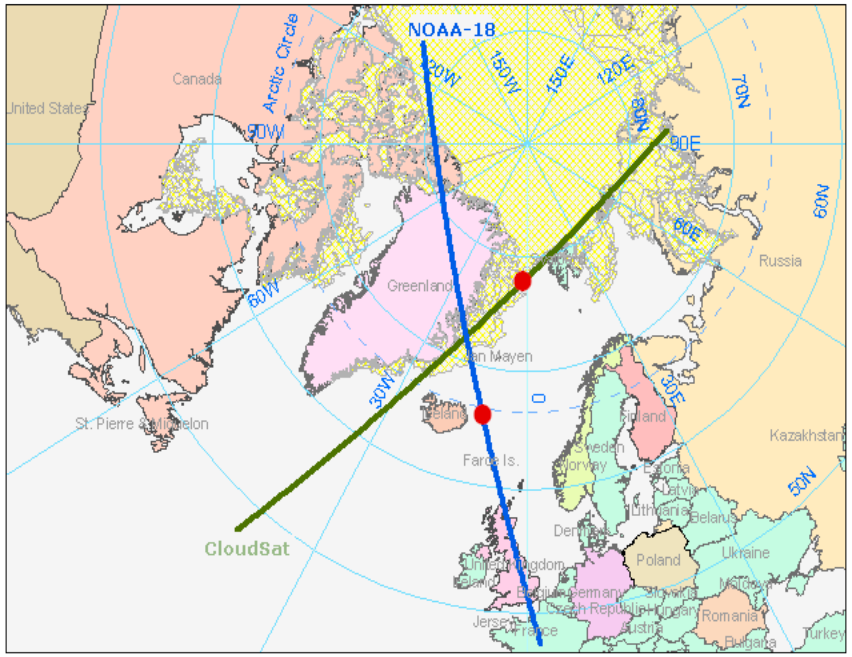

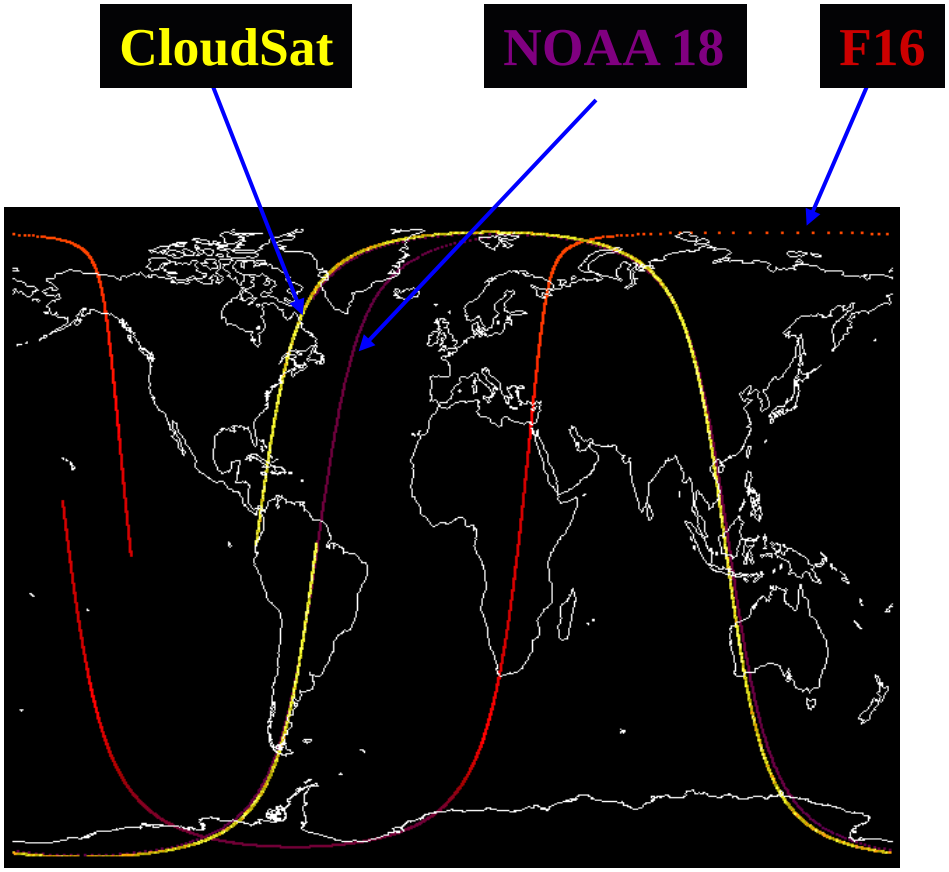

Using SNO method to match the polar-orbiting satellite radiometers.

Matching Criteria for CloudSat and NOAA 18 Data

Spatial distance <
- 50 km AMSUA
- 16 km MHS
- 4 km AVHRR/3

Time difference < 2 minutes

Time periods:
- 07/07/06-08/16/06
- 10/01/06-11/04/06
- 01/01/07-02/01/07

Other constraint: 50°S to 50°N and over ocean

A total of 31 orbit data meet the requirements.

Handling of Cloud Inhomogeneity Effects on CRTM Validation

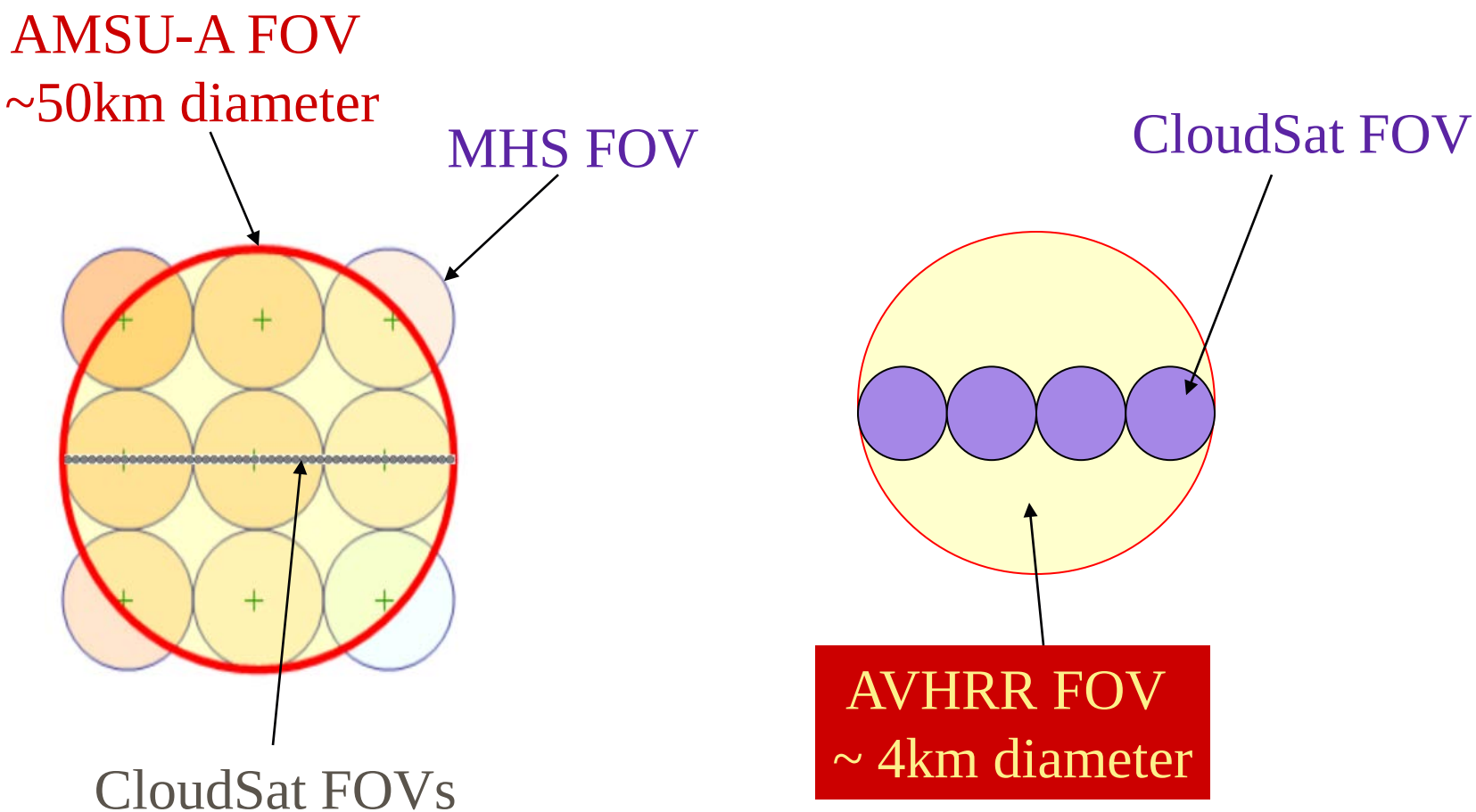

(Chen et al., 2008, JGR)

Assessment of CRTM Cloudy Radiance Simulation Using CloudSat Data

AMSU-A Biases Over Ocean v. s. LWP retrieved by CloudSat

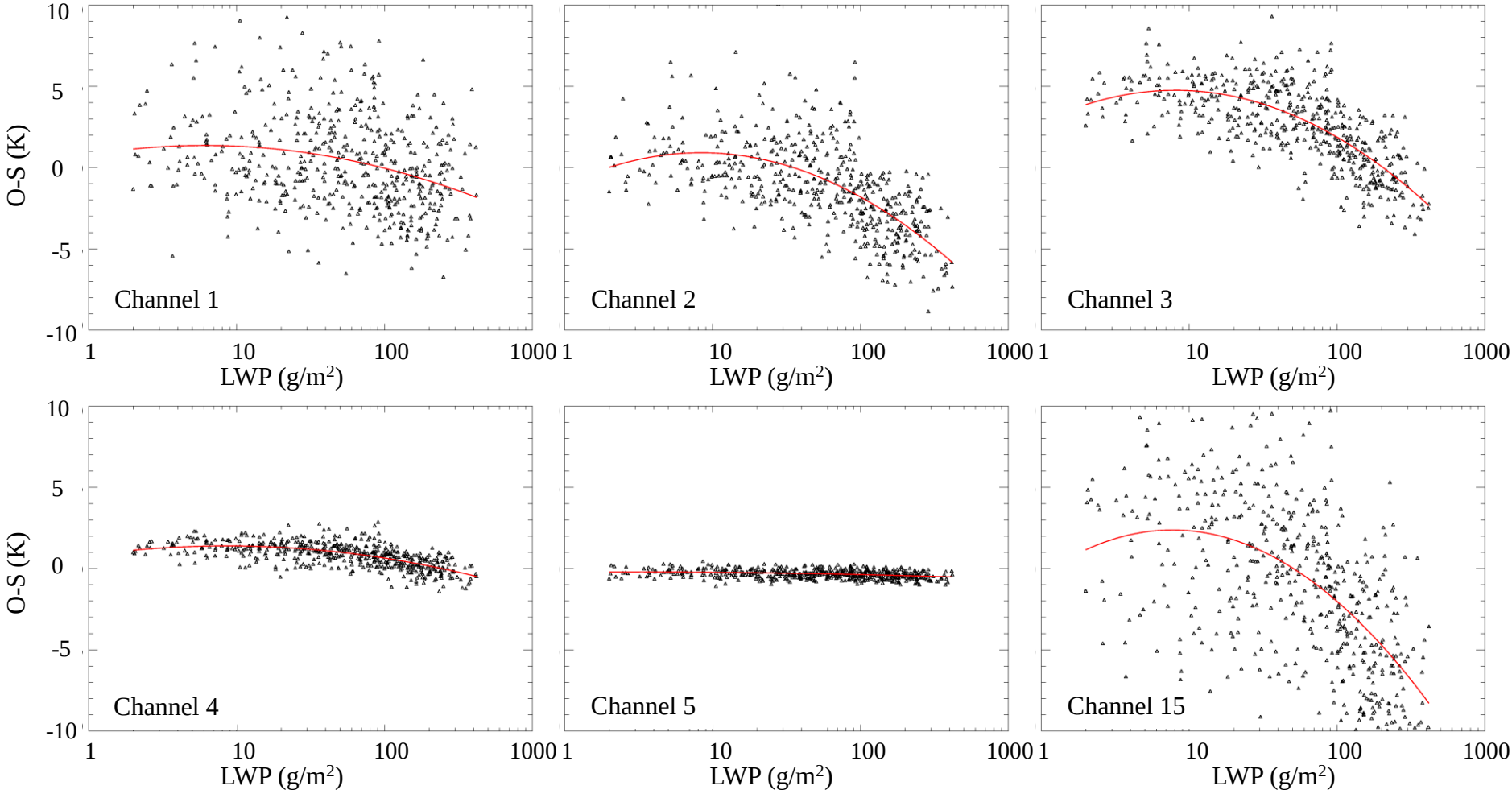

CloudSat provides more accurate hydrometeor profiles used for CRTM inputs. For non-precipitating cloud condition, it is shown that CRTM error increases with Liquid Water Path (LWP) increases for AMSU-A channels 1 to 3.

Observation minus CRTM simulation (O-S) biases over ocean versus LWP retrieved by CloudSat

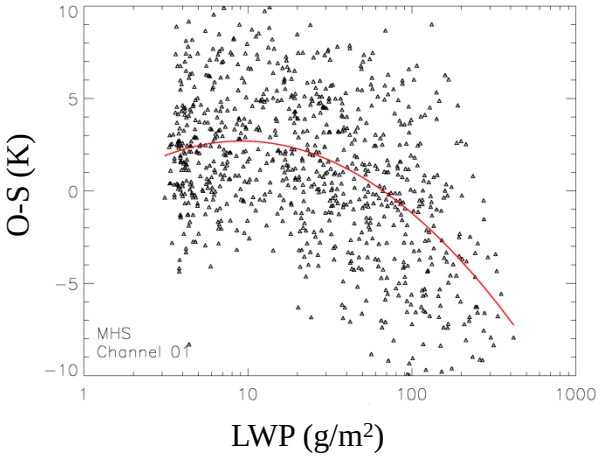

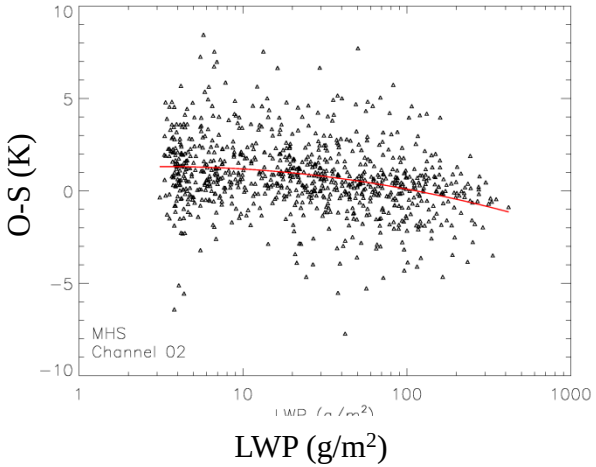

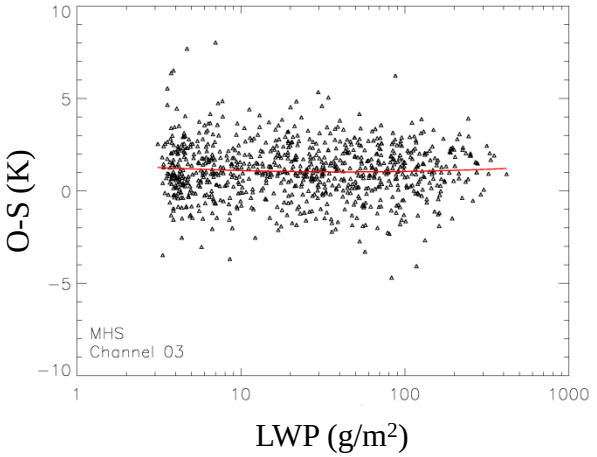

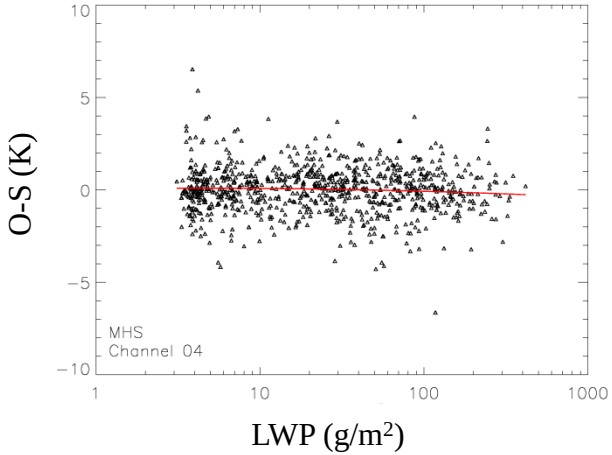

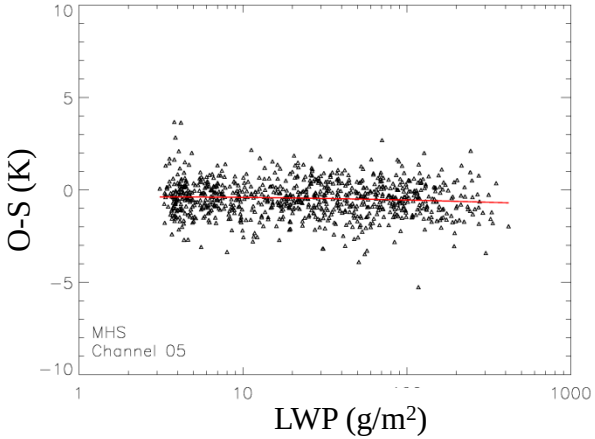

Observation minus CRTM simulation (O-S) biases over ocean versus IWP retrieved by CloudSat

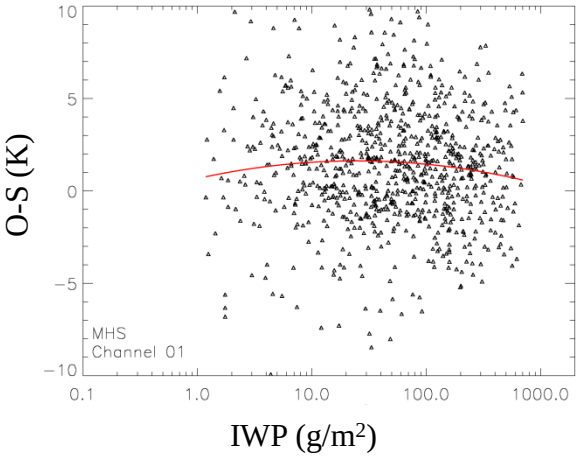

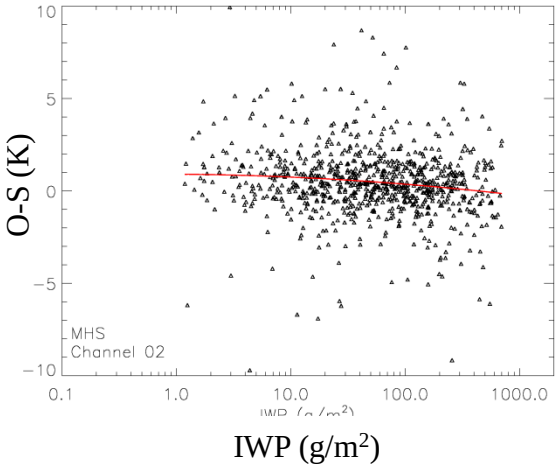

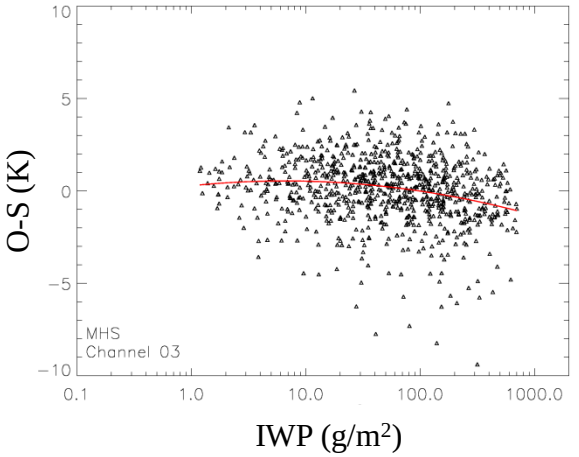

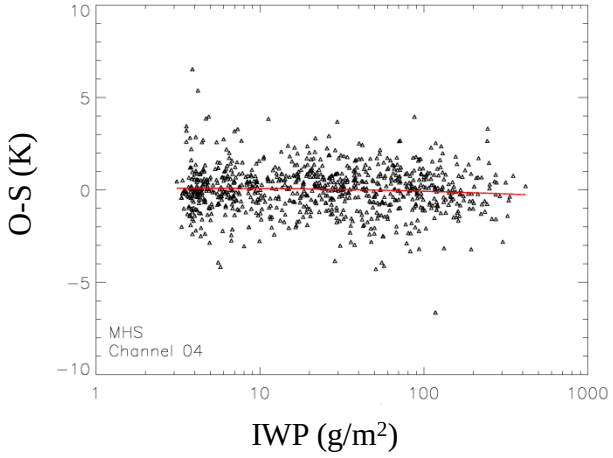

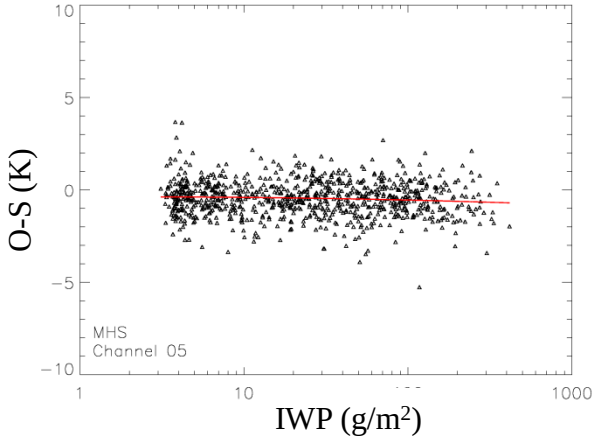

Comparison of Mie Sphere and DDA in RTTOV

- Liu (2008) produced scattering database that contains pre-computed optical properties of non-spherical ice particles, and made it practical to incorporate discrete dipole approximation (DDA) results into fast radiative transfer models for microwave data assimilation.
- Geer and Baordo (2014) implemented Liu's scattering database in RTTOV-SCATT.

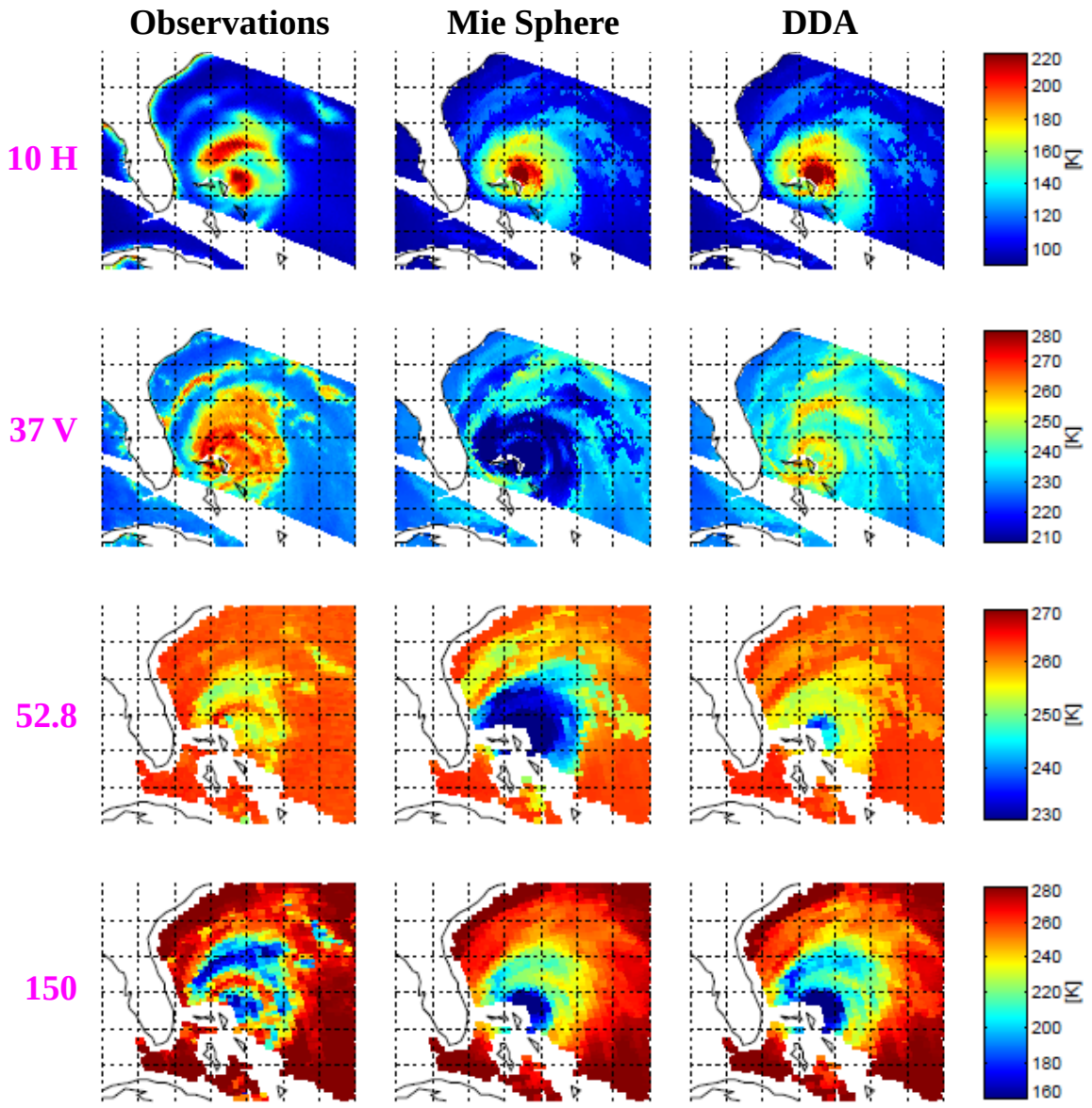

Geer A. J., and F. Baordo, 2014: "Improved scattering radiative transfer for frozen hydrometeors at microwave frequencies", Atmos. Meas. Tech. Discuss., 7, 1749-1805, 2014. DOI:10.519/AMTD-7-1749-2014

GSI Quality Control for AIRS/CrIS/IASI Data

(1) CRTM check
- Reject all channels if CRTM returns an error flag

(2) Satinfo check
- If observation error $e_i > 10^4$, all data are rejected

(3) **Wavenumber check**
- If wavenumber > 2400 and solar zenith angle <= 89, all data over ocean are rejected
- If wavenumber > 2000 and solar zenith angle <= 89, reduce the weight given to data over ocean

(4) Observation check
- If observation>1000 or <=0, all data are rejected

(5) **Cloud check**
- If $\tau_i^K > 0.02$, all data are rejected. τ_i^K Is transmittance at cloud top layer

(6) Surface emissivity/temperature check
- If skin temperature sensitivity related parameter $dts > 1$ and $|\min(dTf, dts) \times ts_i| > max(0.05 \times e_i, 0.02)$ all data are rejected. Value of ts_i depends on surface type
- If skin temperature sensitivity dTf >0.2, all data over land are rejected

(7) Gross check
- If $|T_{B,i}^{Obs} - T_{B,i}^{max} - b_i| > \min(3 \times e_i', e_i^{max})$, all data are rejected. e_i^{max} Is max observation error, b_i is bias correction term.

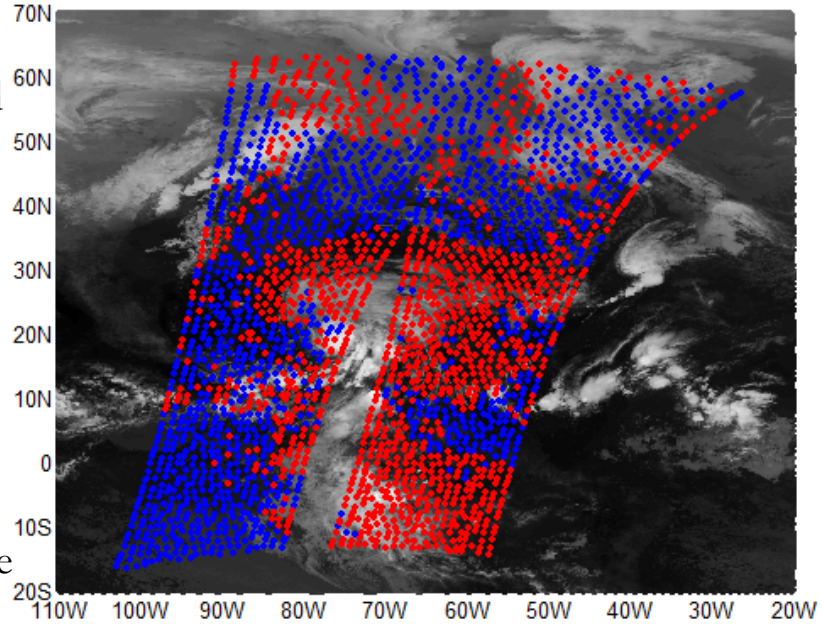

Spatial distribution of CrIS channel 80 data points (699cm-1 ,265hPa) passes all QC check (blue) and failed cloud check (red), background imager shows GOES-13 brightness temperature at 0600 UTC Oct. 26,2012.

Assessments of CRTM NLTE and Solar Reflection at Infrared Shortwave Channels

- Nonlocal Thermal Equilibrium (NLTE) emission at 4.3-mm CO_2 band can be as large as several degrees in Kelvin but is not considered in the current GSI system

- Surface-sensitive shortwave channels (3.5-4.6 mm) are cleaner but not assimilated due to lack of a correction of reflected solar radiance at daytime in the current GSI system

Chen Y., Y. Han, P.-V. Delst, and F. Weng, 2013: Assessment of shortwave infrared sea surface reflection and NLTE effects in CRTM using IASI data. *JTECH*, **30**, 2152-2160.

CRIS O-B w/o NLTE Correction

CrIS Channel 1217 (2330 cm^{-1}, 17 hPa)

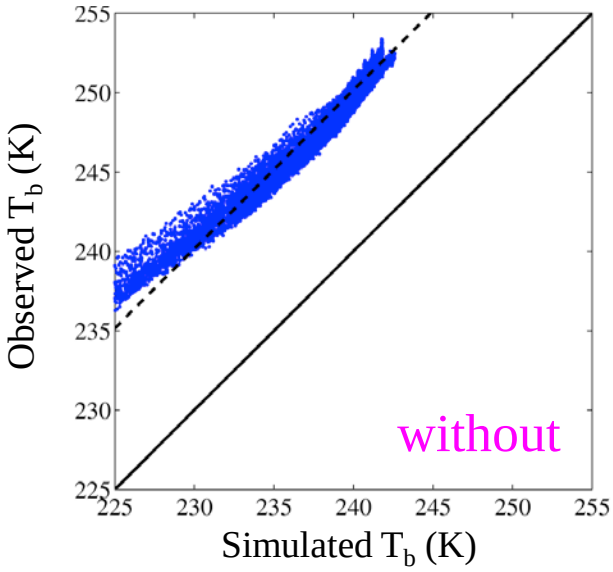

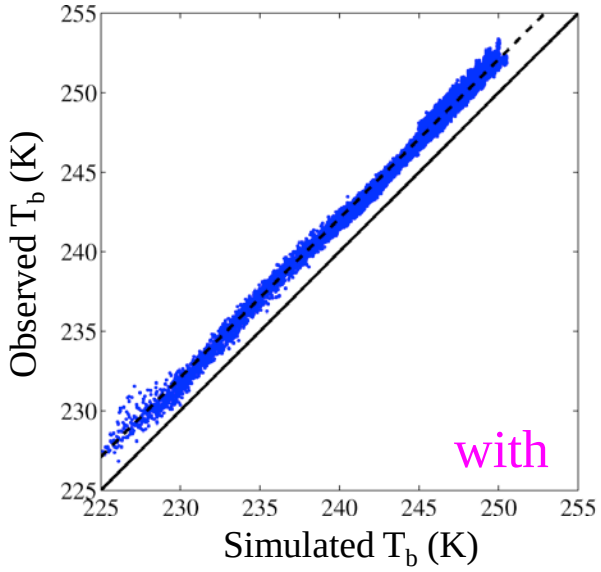

Data over ocean
Ascending node
1800UTC 10/25/12

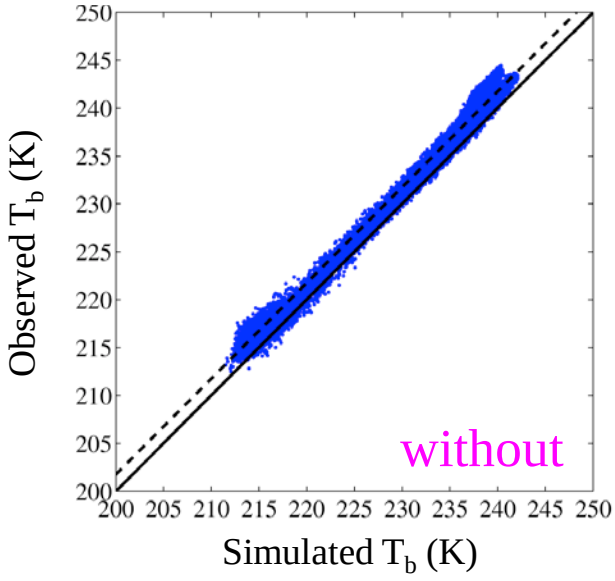

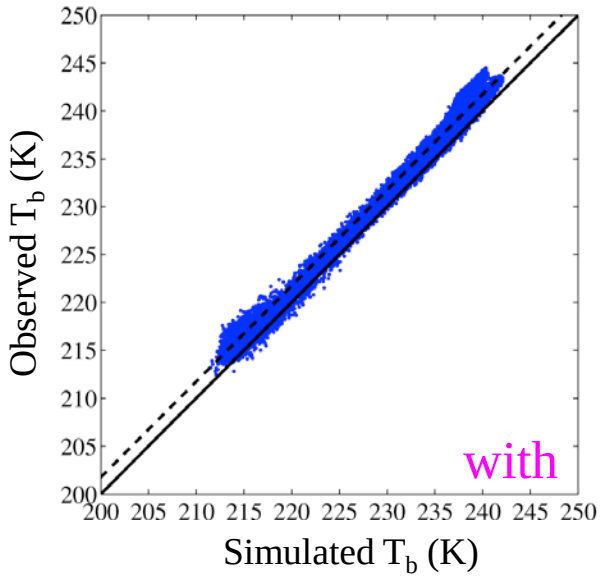

Same channel
Descending node
0600UTC 10/25/12

CrIS SWIR Simulation Including Sun Glint

Shortwave observations over ocean during daytime could be affected by sun glint. Therefore, all data with wavenumbers being larger than 2400 cm^{-1} are removed from assimilation.

However,

Not all CrIS pixels are affected by sun glint!

Percentage VIIRS pixels affected by the sun-glint within each collocated CrIS FOV at 1800 UTC October 25, 2012.

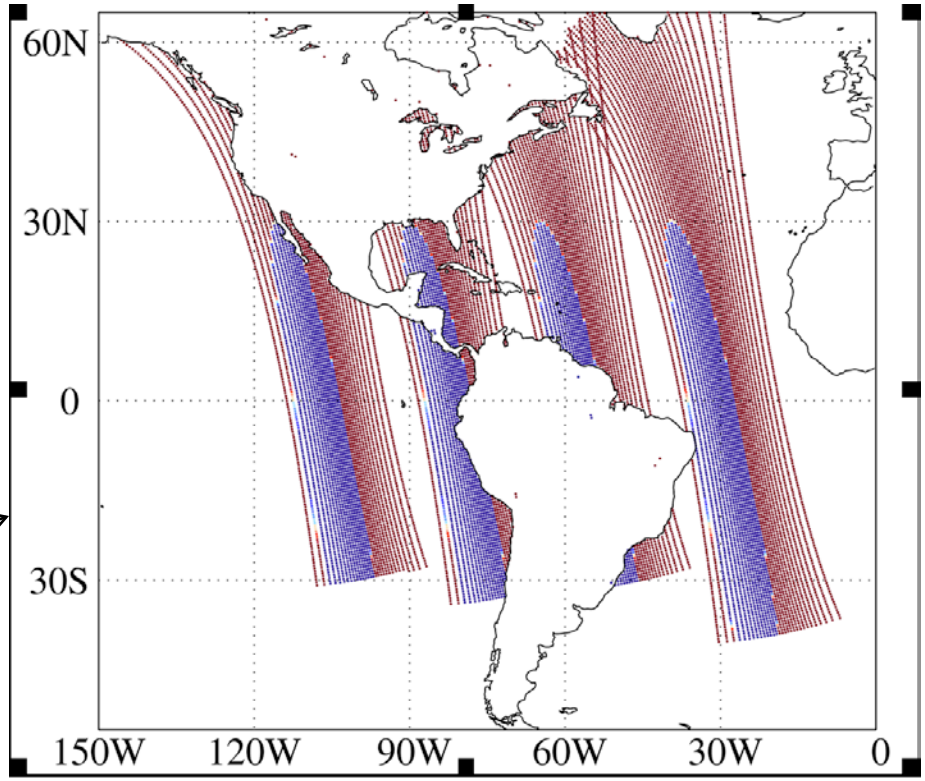

Modified Quality Control Related to Sun Glint

A CrIS pixel is affected by the sun-glint if sun glint angle satisfies

$$0 < \cos^{-1}\left\{\sin\theta_{sat}\sin\theta_{sol}\cos\left[180^{o} - (\phi_{sun} - \phi_{sun})\right] + \cos\theta_{sat}\cos\theta_{sun}\right\} < 36^{0}$$

θ_{sat} – satellite zenith angle θ_{sun} – solar zenith angle

ϕ_{sat} – satellite azimuth angle ϕ_{sun} – solar azimuth angle

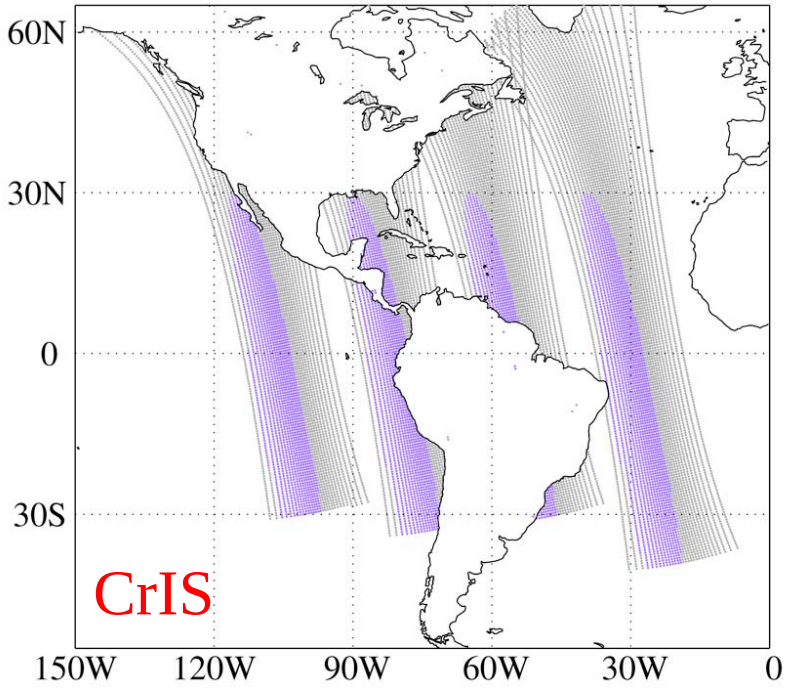

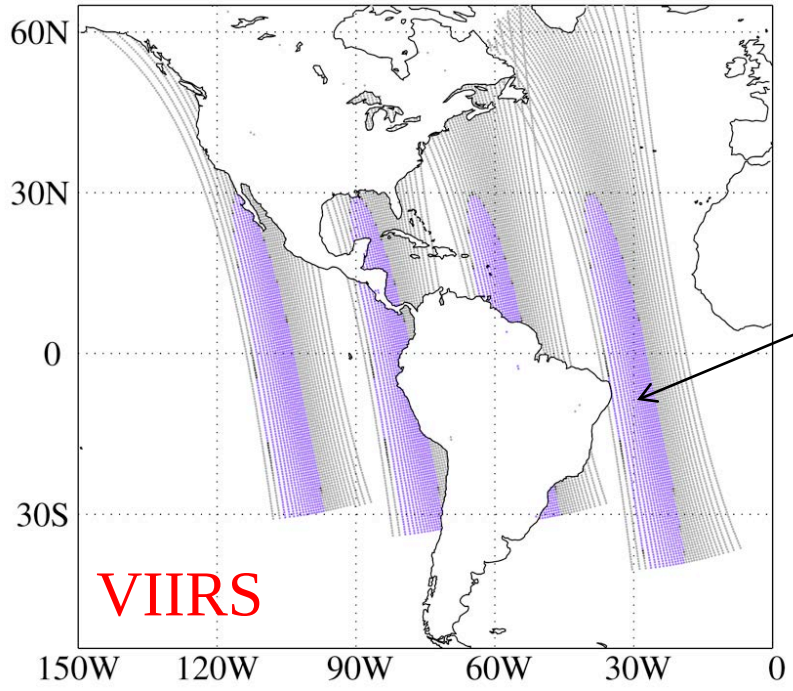

Regions affected by sun glint

CrIS Channel 1293 (2520 cm^{-1}) at FOV5

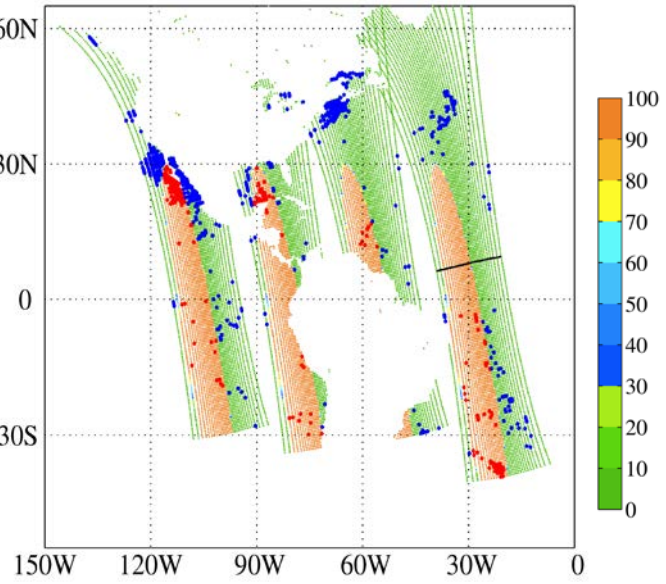

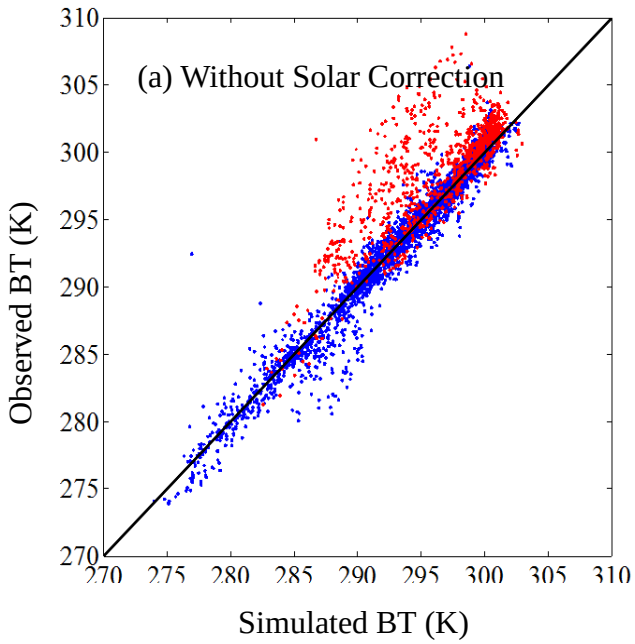

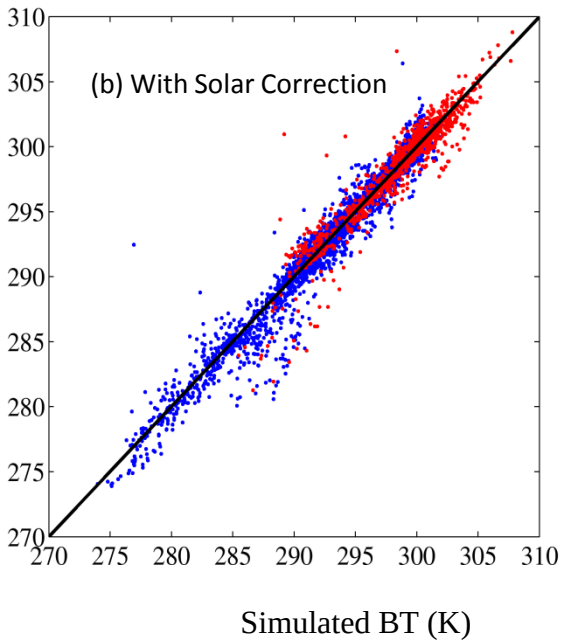

The simulated and observed clear-sky CrIS channel 1293 (wavenumber 2520.0) FOV5 brightness temperature of the same dots shown in Fig.1 at 1800 UTC Oct 25, 2012 (a) without solar correction, and (b) with solar correction. The CrIS FOV5 observations within which 99.9%, and 0.1% of collocated VIIRS pixels are affected by sun-glint are respectively shown in red, and blue.

CRIS O-B Biases w/o NLTE Correction

Ascending node, clear-sky data over ocean at 1800UTC during 22-29 October 12

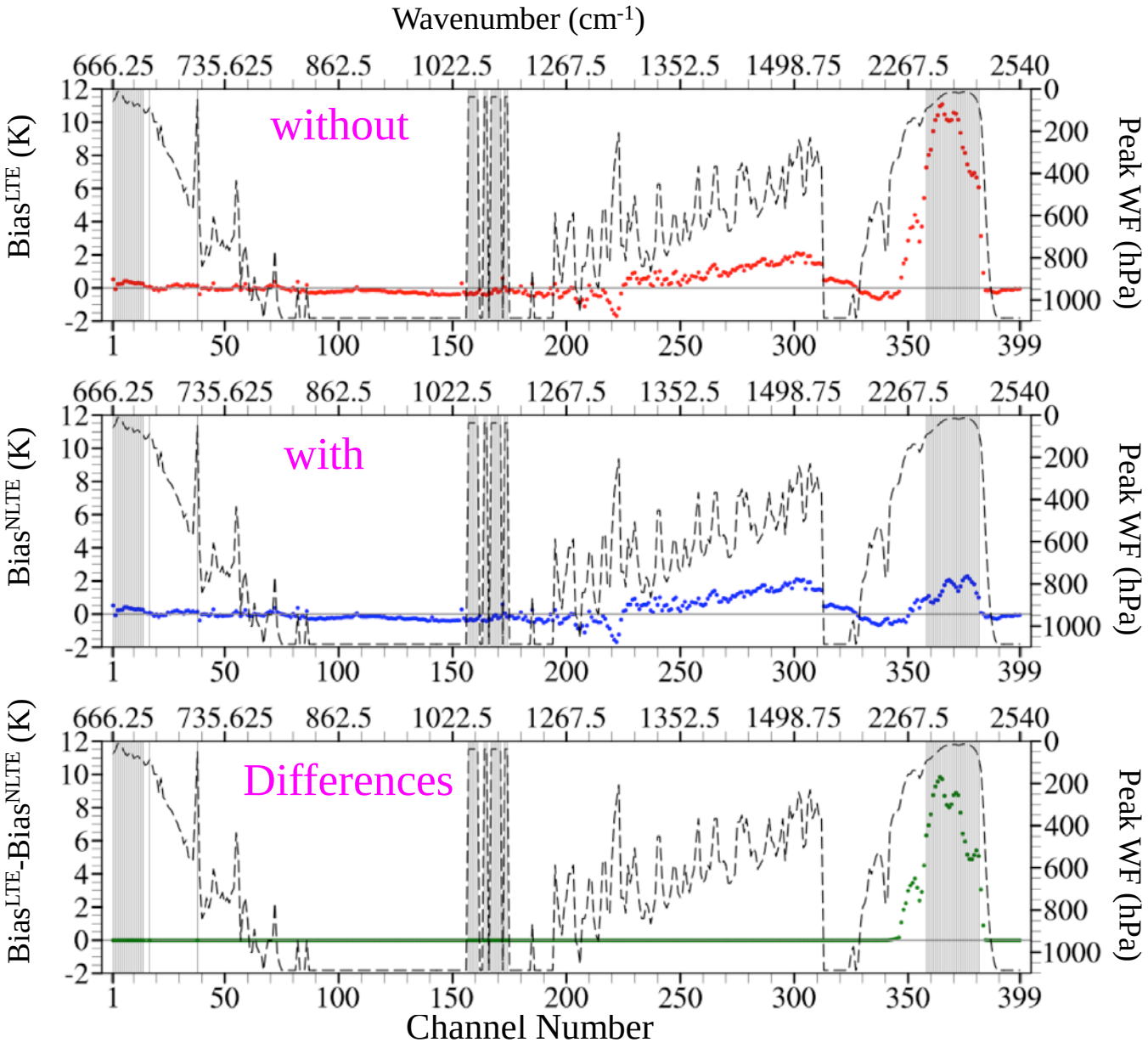

Biases are indicated by colored dots.

Pressure levels at which WF peaks are indicated by the black dashed line.

Channels with WF peaks higher than 100 hPa are indicated by the gray vertical lines.

CRIS O-B Biases w/o Solar Correction

Ascending node, clear-sky data over ocean at 1800UTC during 22-29 October 12

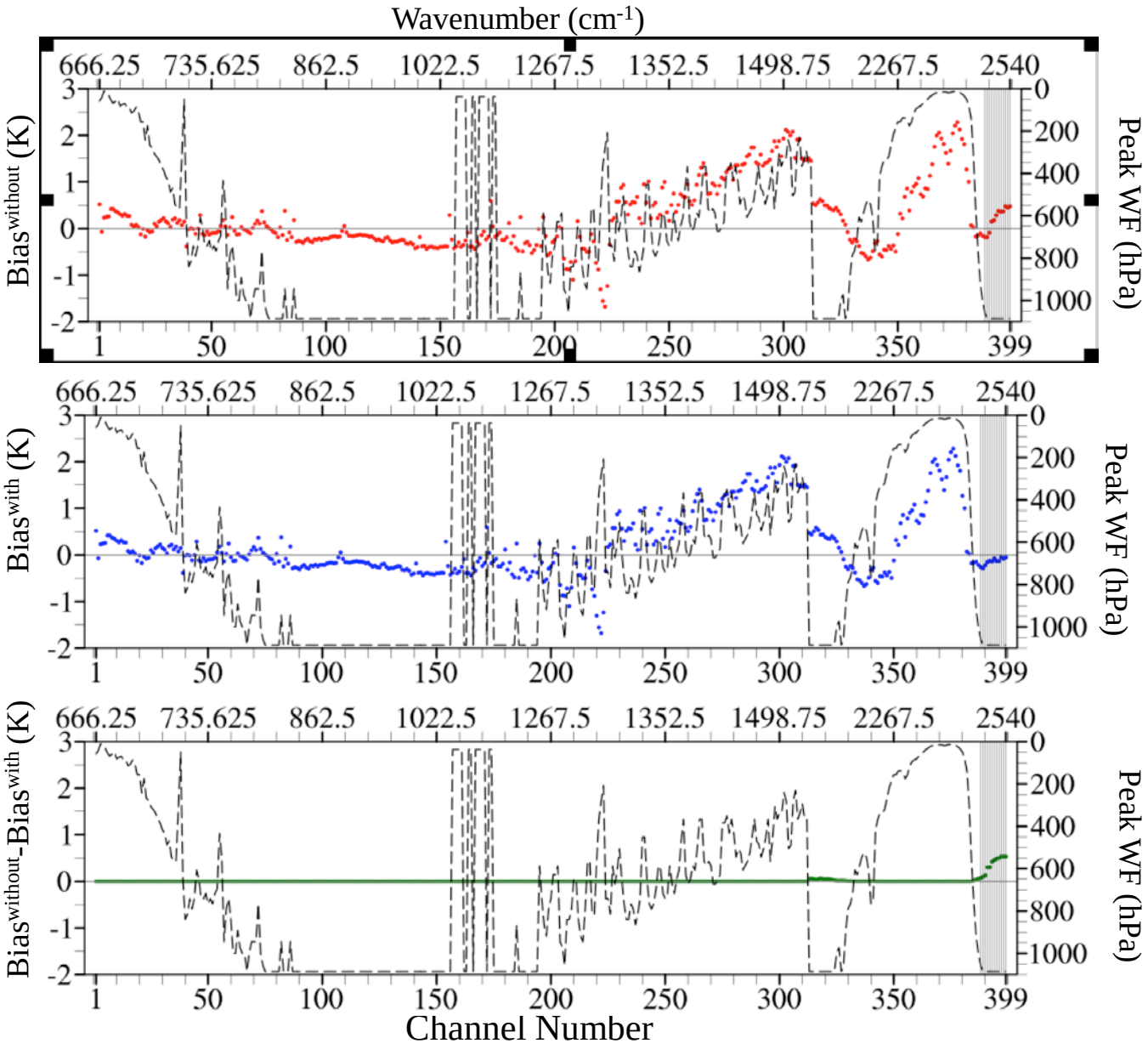

Biases are indicated by colored dots.

Pressure levels at which WF peaks are indicated by the black dashed line.

Channels with wavenumbers greater than 2400 μm are indicated by the gray vertical lines.

Radiometer measurements from satellite and wind vector from NWP

From Masahiro Kazumori, presentation in 2013 EUMESAT Satellite Conference

AMSR-E 19GHz V

Wind Speed

6 [m/s] | 10 [m/s] | 12 [m/s] | 14 [m/s]

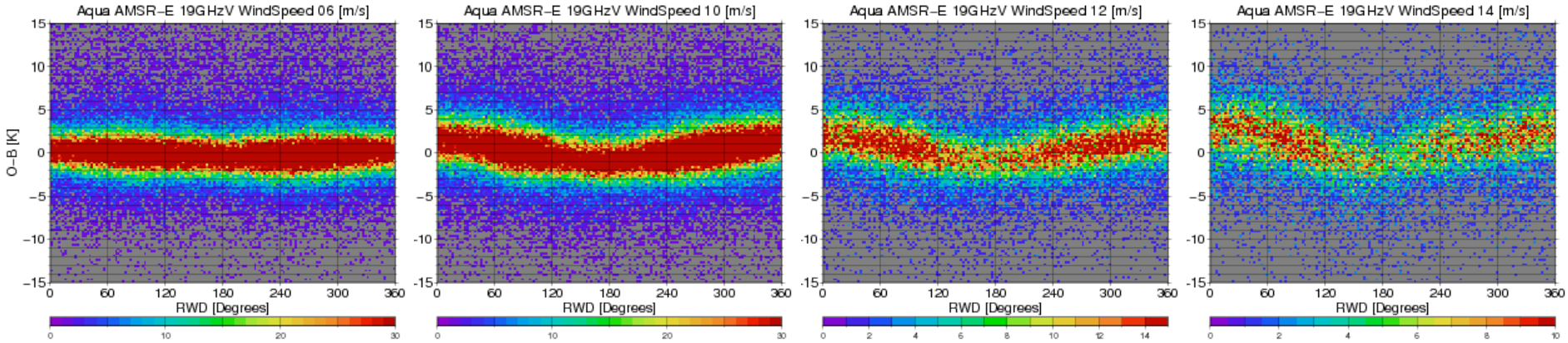

AMSR-E 19GHz H

Wind Speed

6 [m/s] | 10 [m/s] | 12 [m/s] | 14 [m/s]

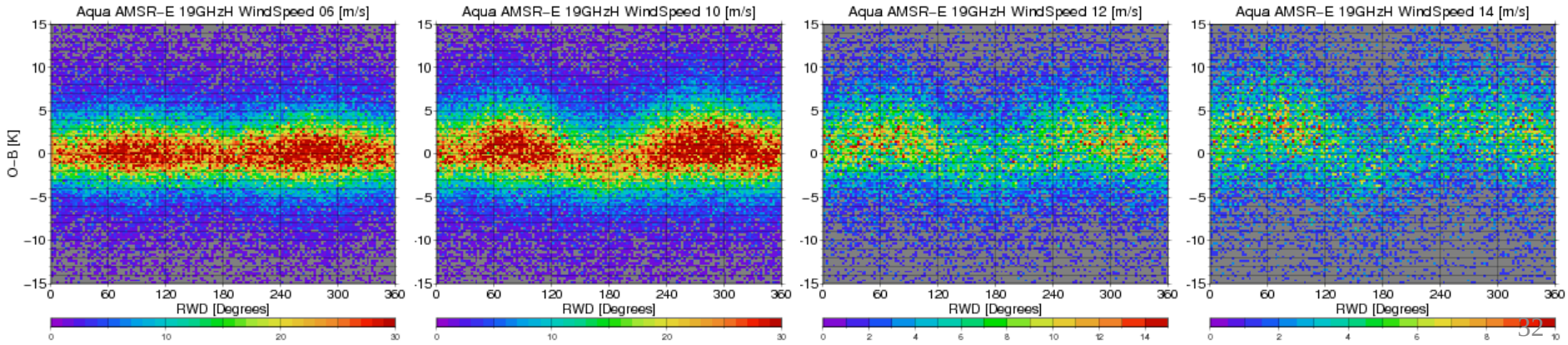

FASTEM-5 Simulations

In this study we compare azimuthal angle-dependent feature of Fastem-5 in CRTM and RTTOV. Inputs to FASTEM come from GDAS sea surface temperature and wind speed/direction.

Fastem-5 in RTTOV10.2 run by Kazumori

Fastem-5 in CRTM 2.1, $Revision: 17159

No atmosphere being considered in the simulation

Parameters	Value
AMSR2 Frequency (GHz)	10.65, 18.7, 23.8, 36.5, 89
Satellite Zenith Angle (deg)	55
Satellite Azimuth Angle(deg)	0~360
Wind Speed (m/s)	6, 9, 12, 15, 18
Wind Direction (deg)	0
Sea Surface Temperature (K)	270~300

MW Ocean Emissivity Including the RWD Effect

- Ocean surface radiations have surface wind directional signals.
- The azimuthal variation correction for **R**elative **W**ind **D**irection (RWD) effect should be handled properly in radiative transfer calculation for radiance assimilations.

Variations of ΔT_b Simulated by FASTEM5 (SSMIS 19.35 GHz)

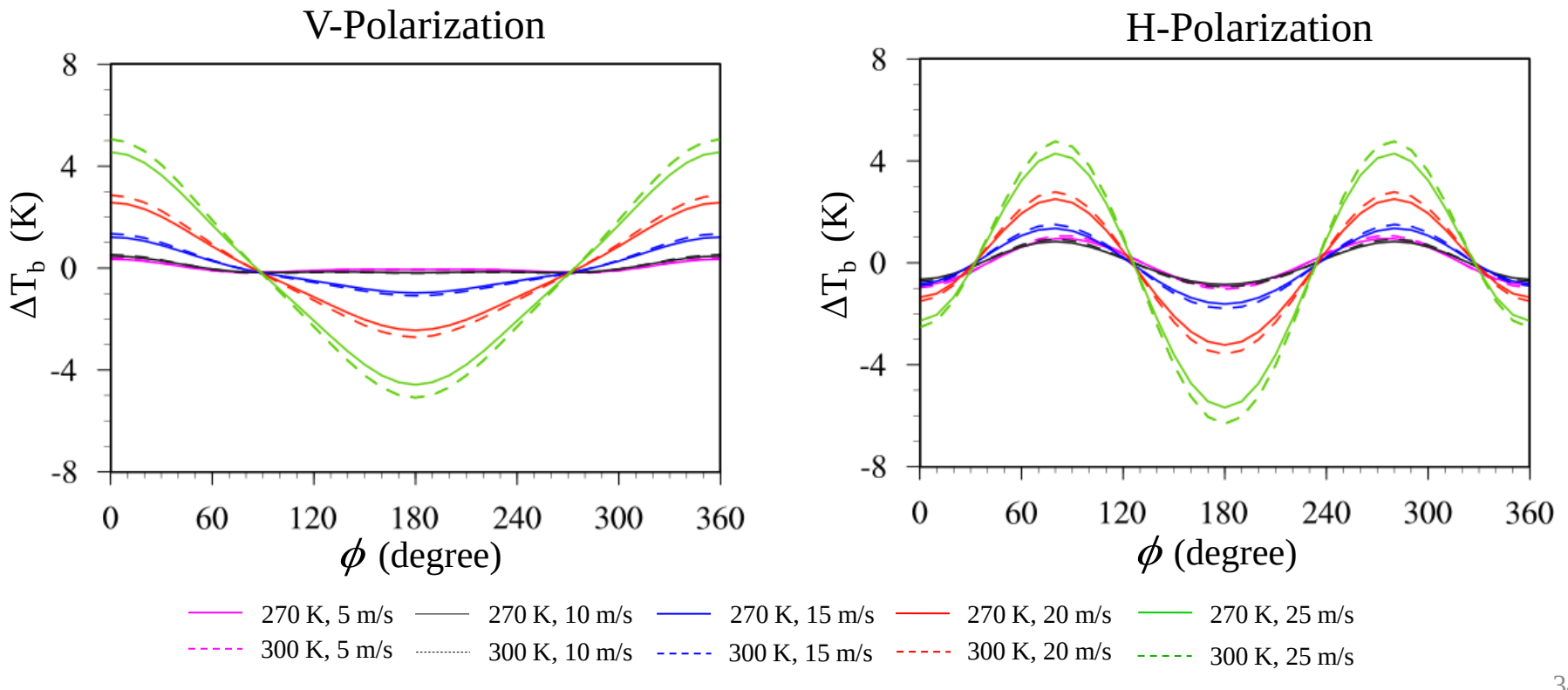

Benefits of Vector RTM for Conical Scan MW Imager

AMSR2 Azimuth Angle (Deg)

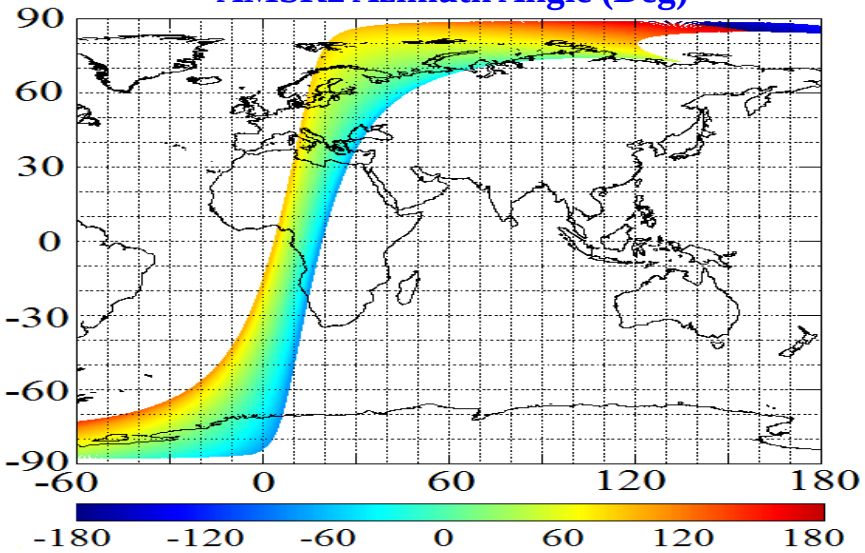

Relative Wind Direction (Deg)

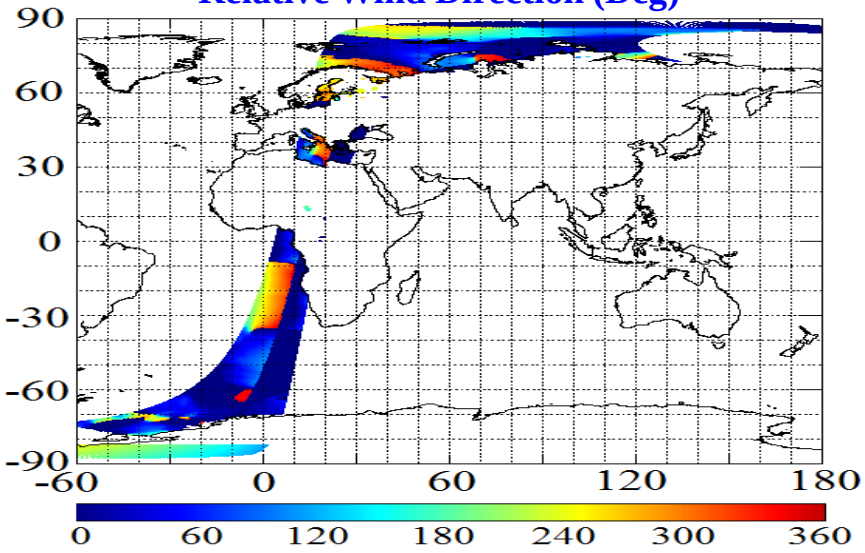

TB Difference at 10GHz V (K)

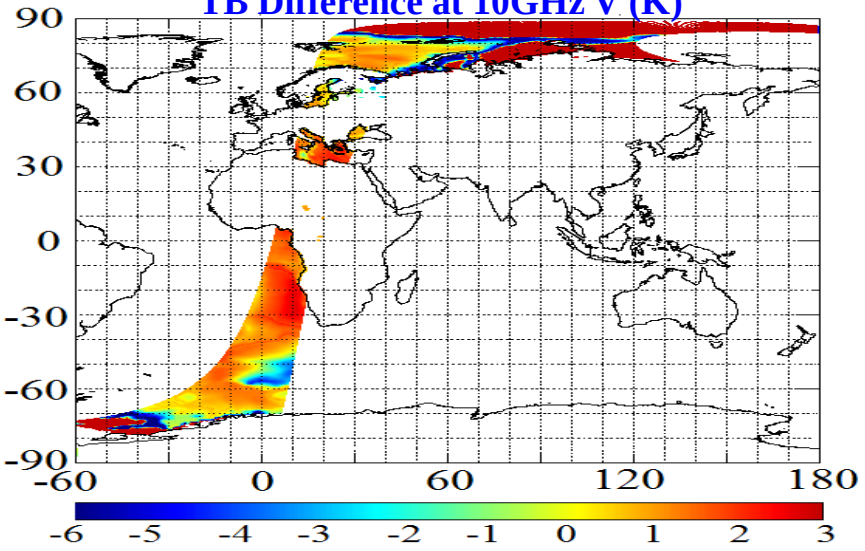

TB Difference at 10GHz H (K)

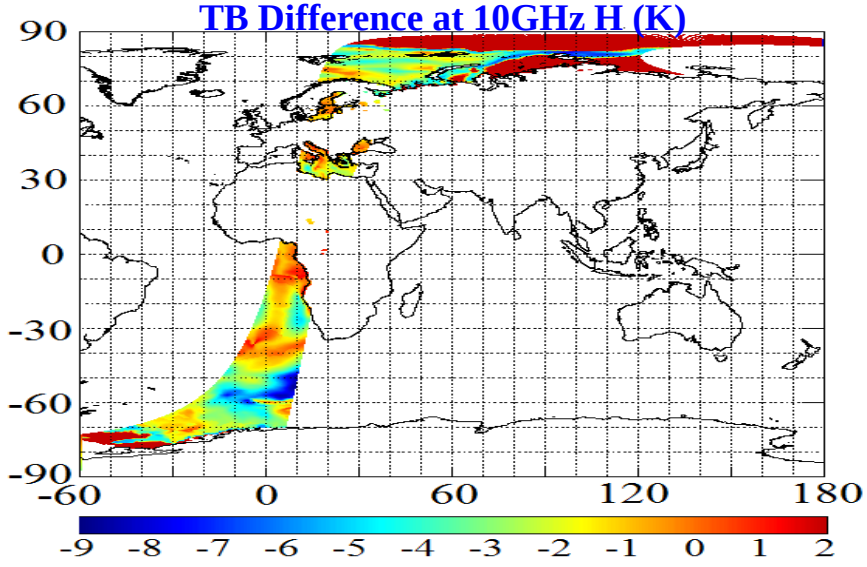

The RWD effect can lead up to a few degree difference in the brightness temperature simulation over ocean for AMSR2.

Simulated vs. Observed Azimuthal Dependence of Brightness Temperature at 18.7 GHz V-pol

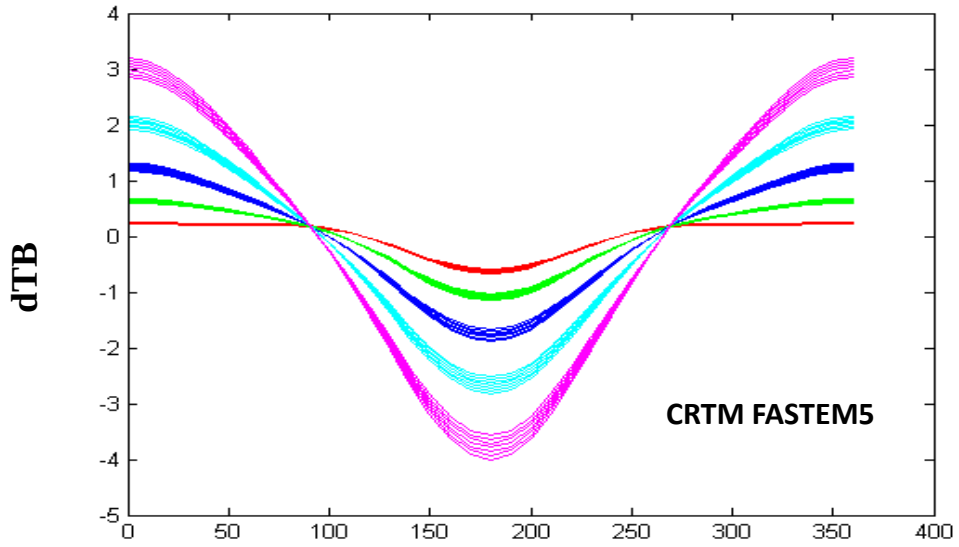

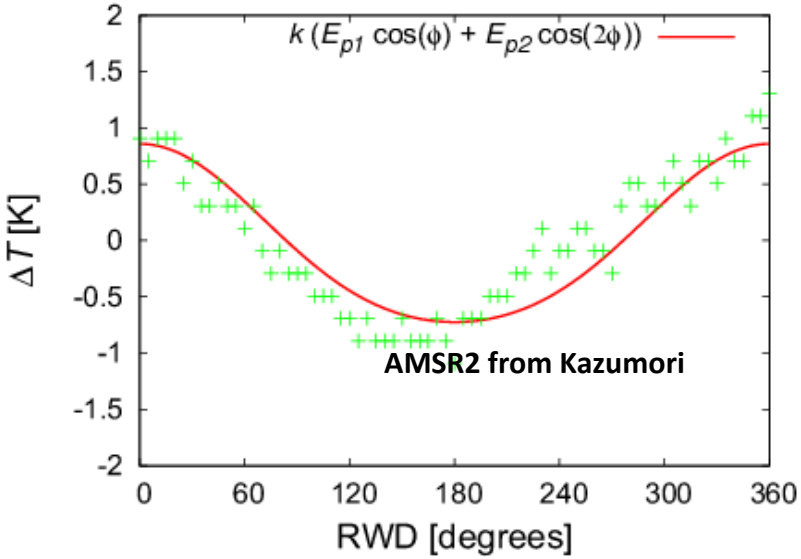

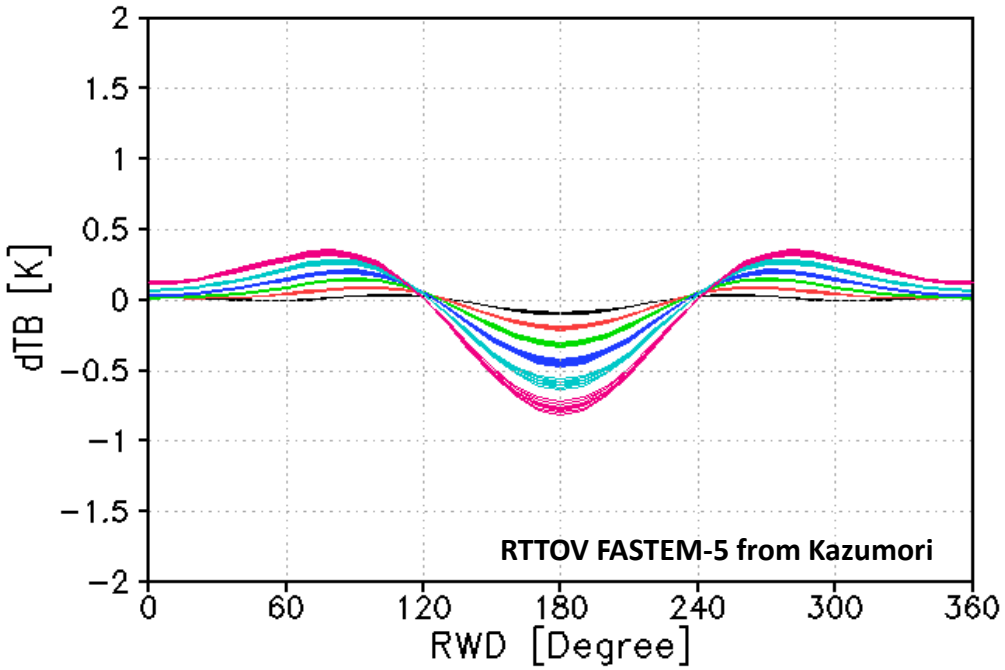

6m/s
9m/s
12m/s
15m/s
18m/s

Simulated vs. Observed Azimuthal Dependence of Brightness Temperature at 18.7 GHz H-pol

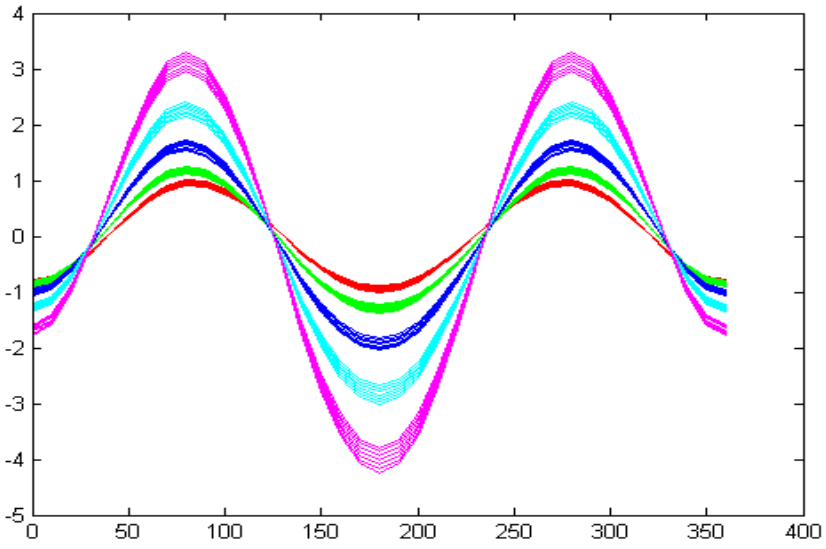

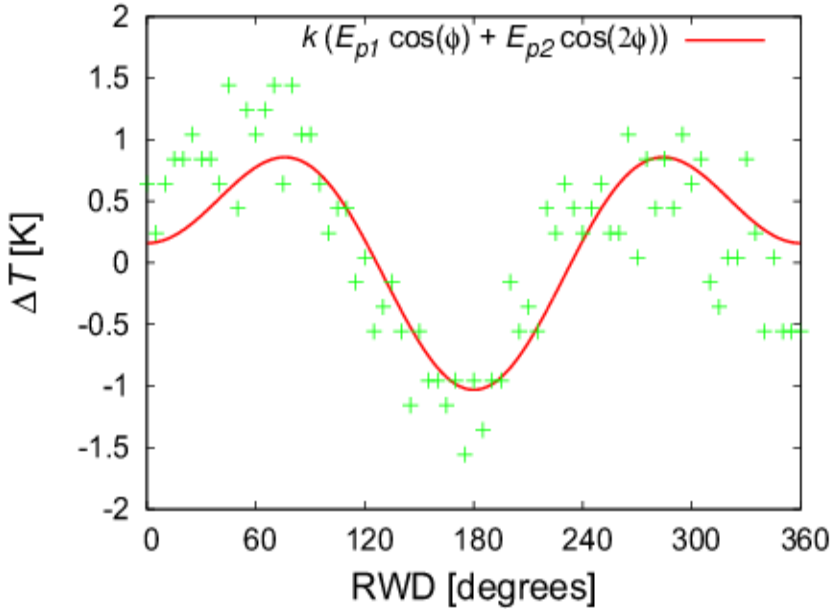

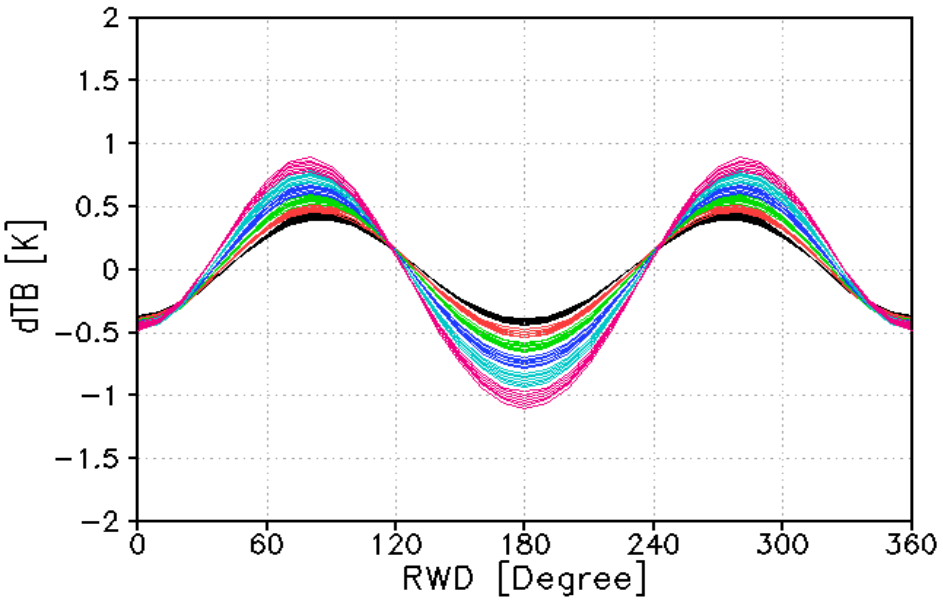

6m/s
9m/s
12m/s
15m/s
18m/s

ATMS SDR Scan Angle Dependent Bias

- **Methodology:**
  - SDR angular dependent biases are assessed using ECMWF and CRTM simulations
  - Cloud-affected radiances are removed with cloud liquid water algorithm (Weng et al., 2003)
  - Also, the measurements with the surface wind speeds are less than 10m/s are used
- **Results:**
  - ATMS SDR sounding channels have small bias but less angular dependent
  - But window channels have some significant biases

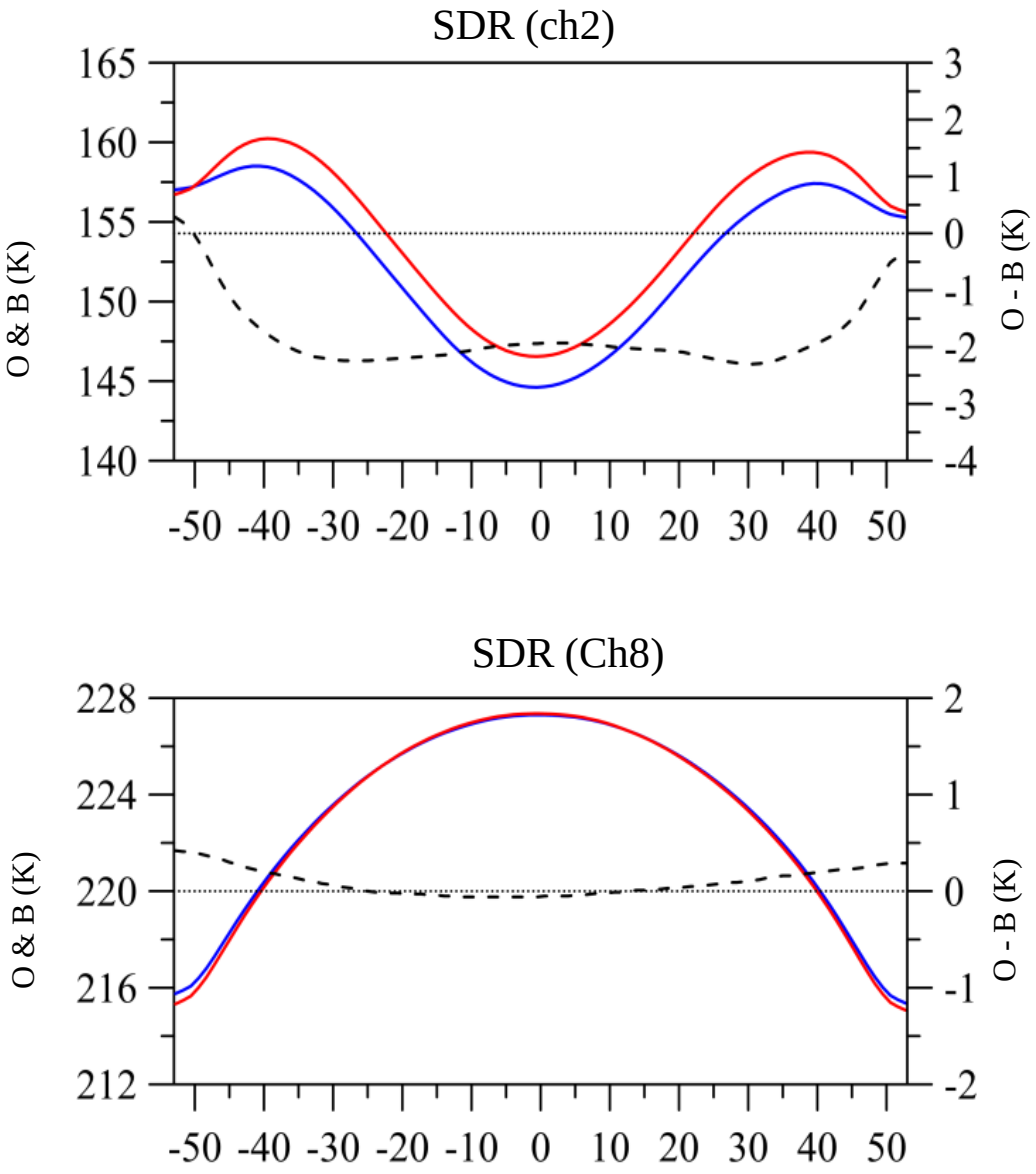

ATMS Scan Dependent O-B (TDR vs. SDR)

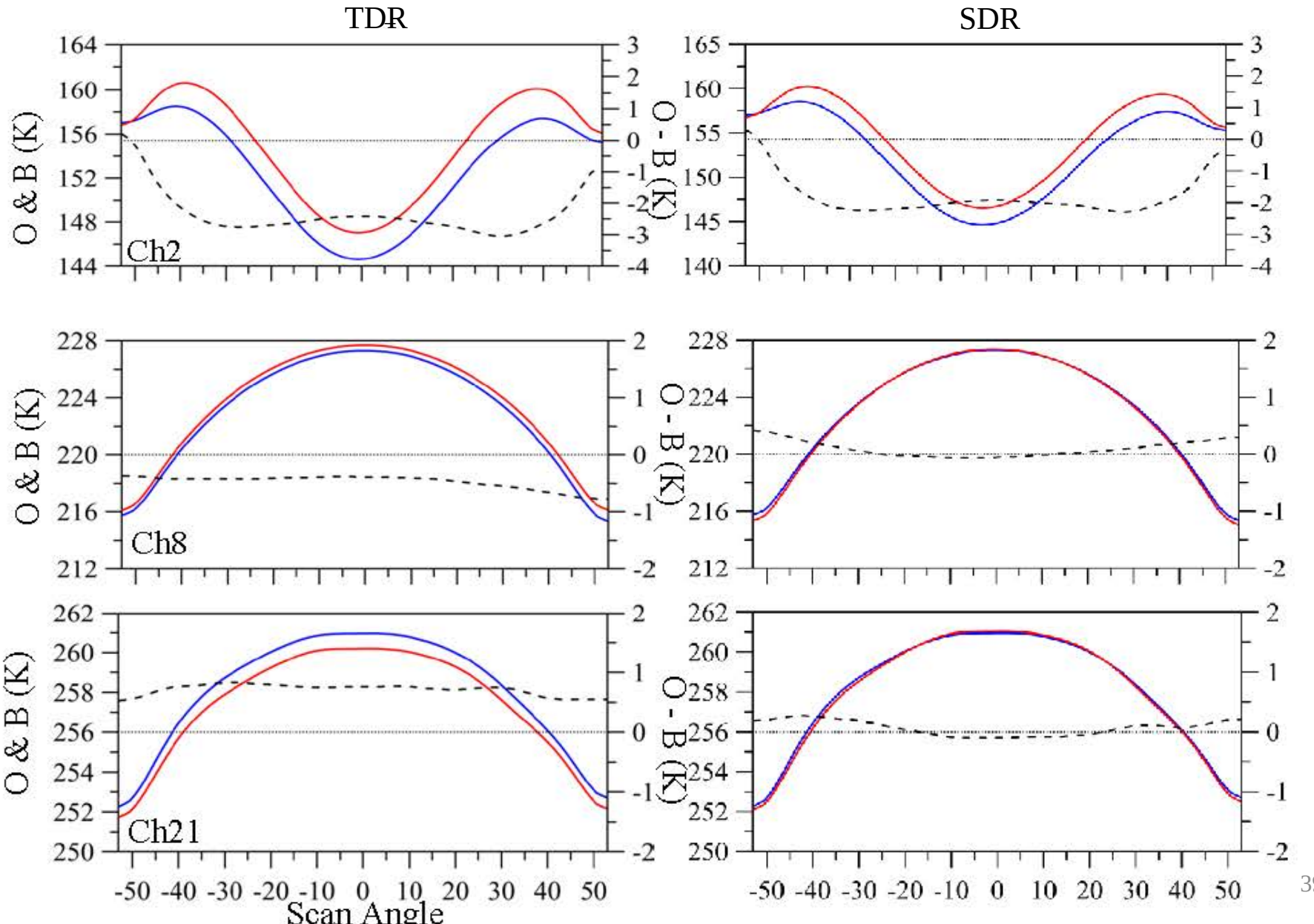

ATMS SDR Biases due to The 3rd Stokes Component

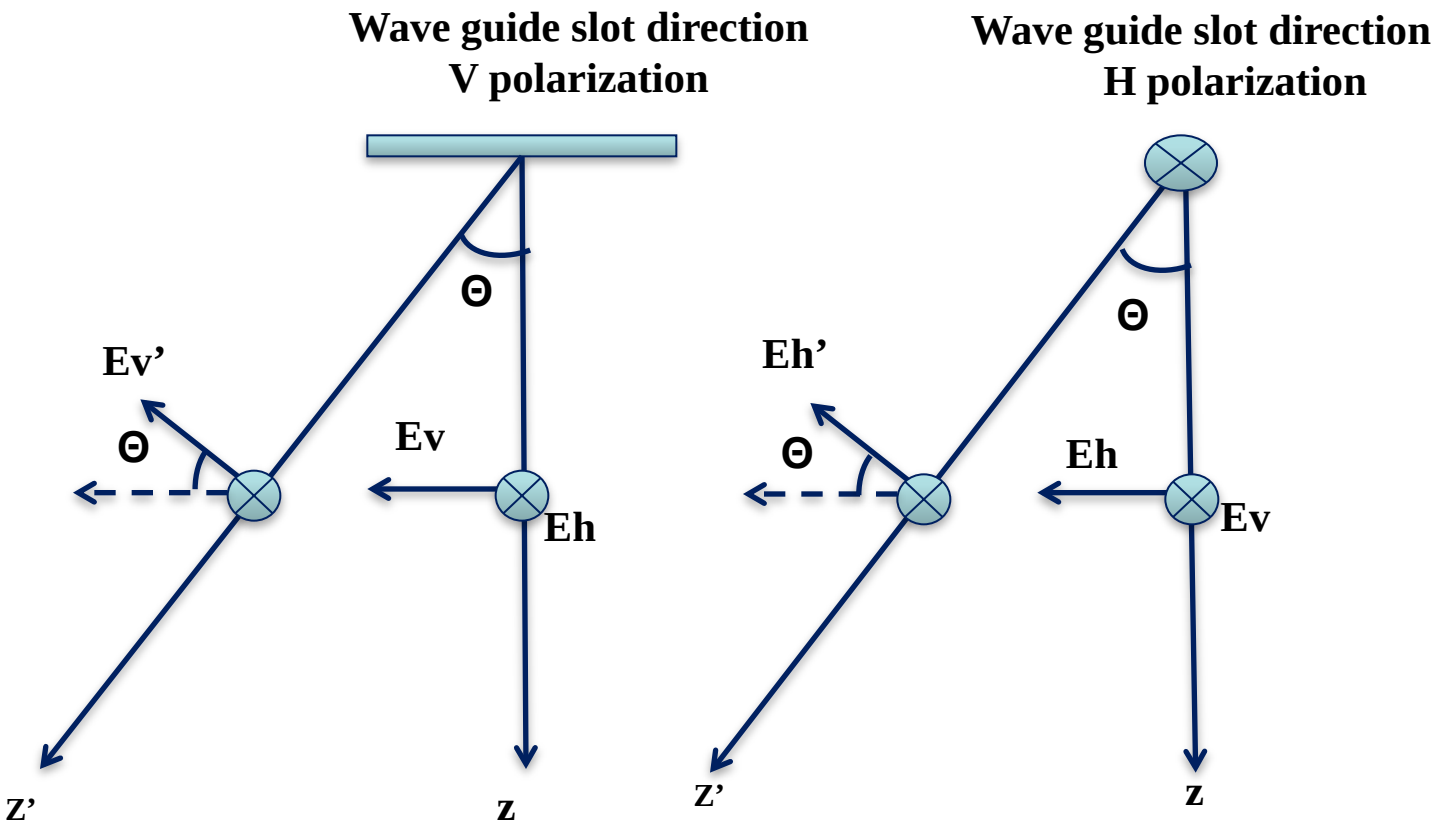

Eh vector is defined as the electronic vector perpendicular to wave propagation plane

$$\begin{bmatrix} T_B^{QV} \\ T_B^{QH} \\ T_B^{Q3} \\ T_B^{Q4} \end{bmatrix} = \begin{bmatrix} cos^2\theta & \sin^2\theta & 0.5\sin 2\theta & 0 \\ \sin^2\theta & cos^2\theta & -0.5\sin 2\theta & 0 \\ -\sin 2\theta & \sin 2\theta & \cos 2\theta & 0 \\ 0 & 0 & 0 & 1 \end{bmatrix} \begin{bmatrix} T_B^V \\ T_B^H \\ T_B^3 \\ T_B^4 \end{bmatrix}$$

$$T_B^{QV} = T_B^H \sin^2\theta + T_B^V \cos^2\theta + T_b^3 \frac{1}{2}\sin 2\theta$$

$$T_b^{QH} = T_b^H \cos^2\theta + T_b^V \sin^2\theta - T_b^3 \frac{1}{2}\sin 2\theta$$

Benefits of Vector RTM for Cross-Track Scanning MW Sounder

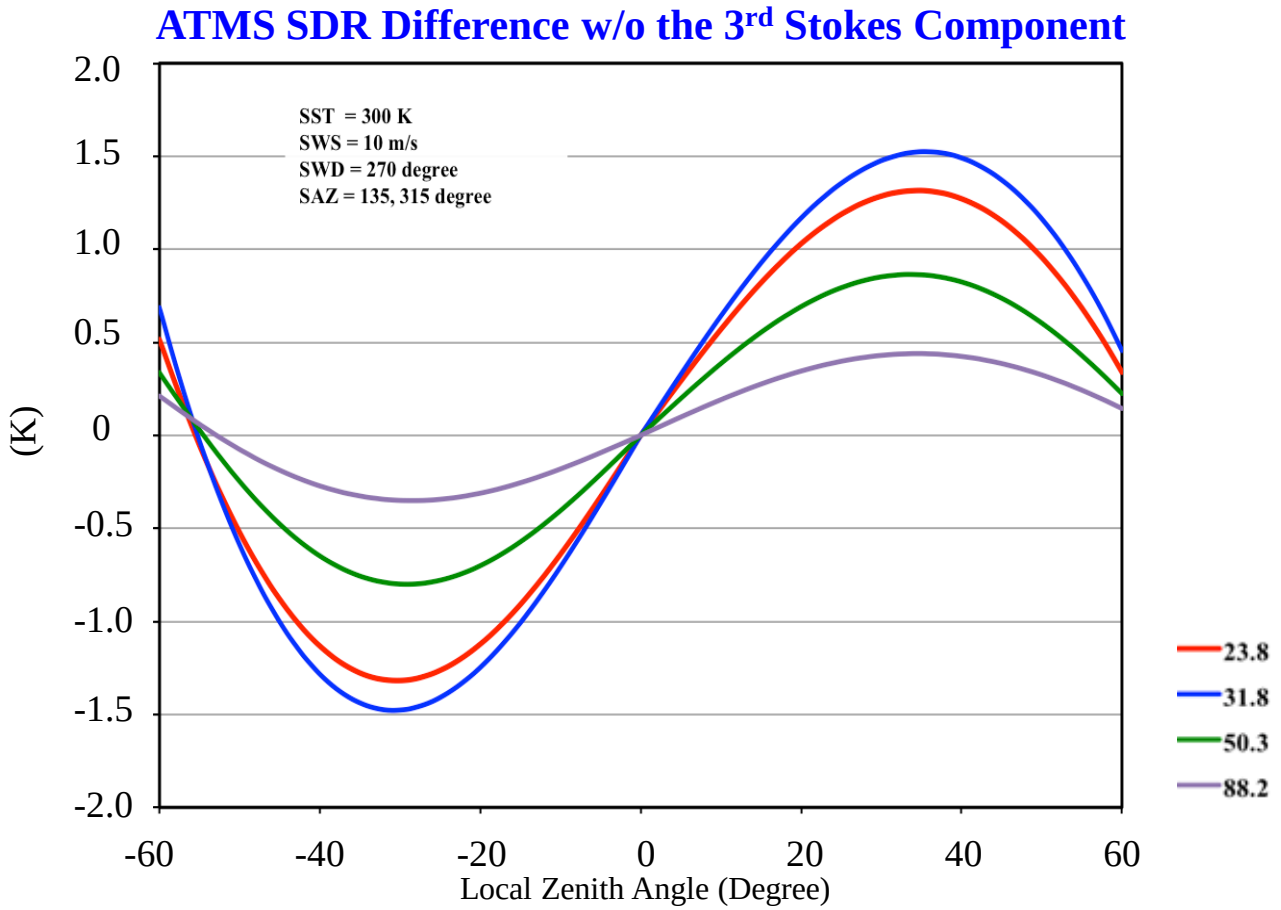

- For accurate simulation of surface sensitive channels over polarized surfaces, such as ocean surface, and considering the fact that ATMS window channels are also affected by the 3rd Stokes component, it is important to properly simulate all these effects.
- These effects can be only handled through vector RTM.

ATMS TDR Simulations

For Quasi-V (TDR) :

$$T_a^{Qv} = \eta_{me}^{vv} T_b^{Qv} + \eta_{me}^{hv} T_b^{Qh} + \eta_{se}^{vv} T_{b,se}^{Qv} + \eta_{se}^{hv} T_{b,se}^{Qh} + (\eta_{sc}^{vv} + \eta_{sc}^{hv}) T_{c,RJ} + S_a^{Qv}$$

For Quasi-H (TDR)

$$T_a^{Qh} = \eta_{me}^{hh} T_b^{Qh} + \eta_{me}^{vh} T_b^{Qv} + \eta_{se}^{hh} T_{b,se}^{Qh} + \eta_{se}^{vh} T_{b,se}^{Qv} + (\eta_{sc}^{hh} + \eta_{sc}^{vh}) T_{c,RJ} + S_a^{Qh}$$

Weng, F., *X. Zou, M. Tian, W.J. Blackwell, N. Sun, H. Yang, X. Wang, L. Lin, and K. Anderson, 2013, Calibration of Suomi National Polar-Orbiting Partnership (NPP) Advanced Technology Microwave Sounder (ATMS), J. Geophys. Res,* ***118****, 1–14, doi:10.1002/jgrd.50840 ,*

ATMS Polarization vs. Scan Angle

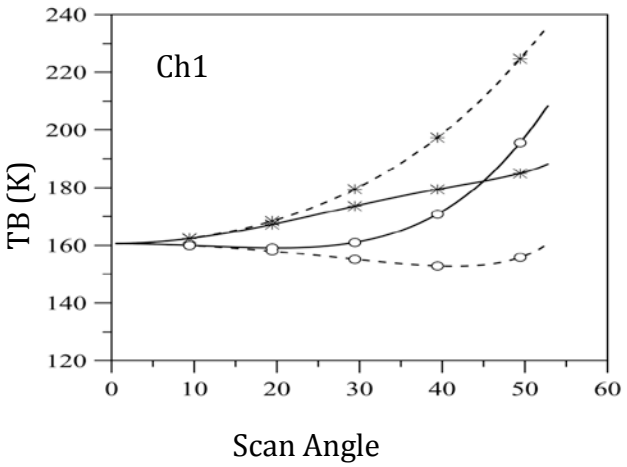

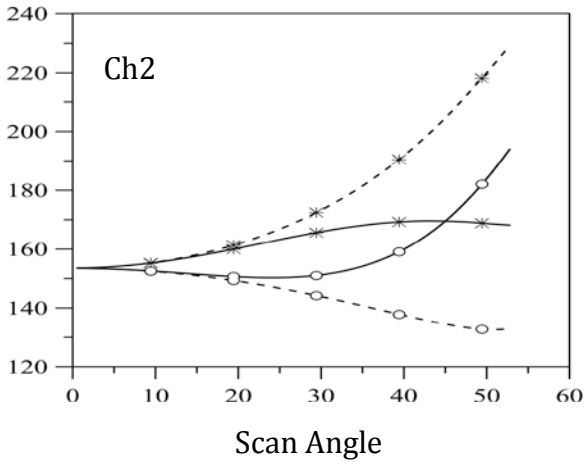

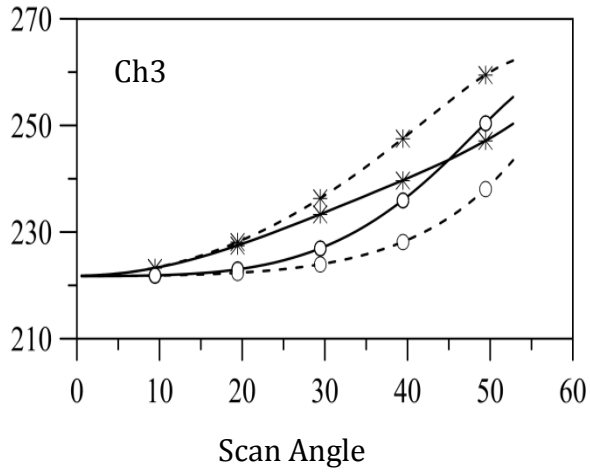

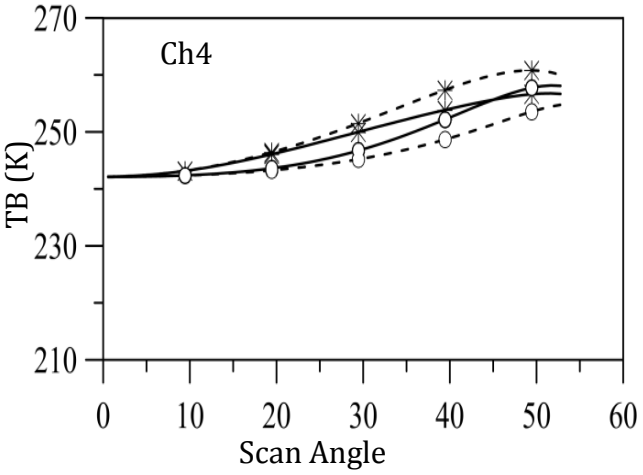

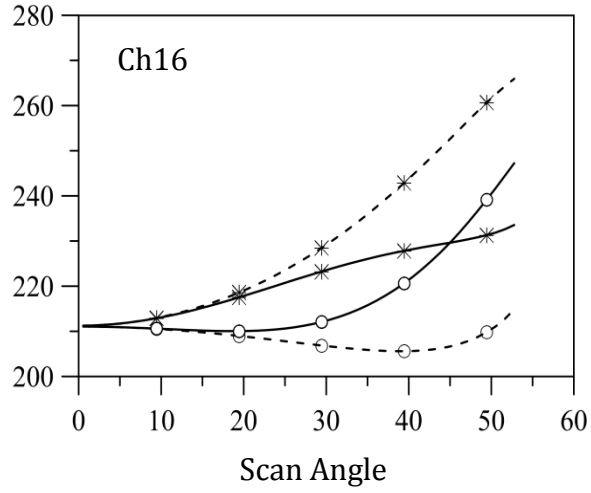

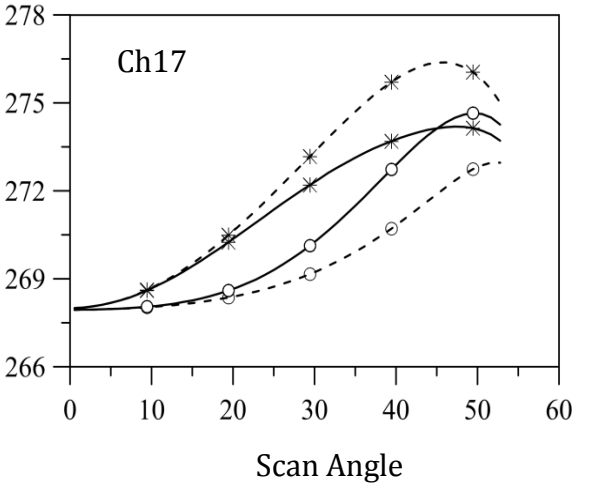

The brightness temperature with pure (dashed curve) and quasi- (solid curve) horizontal polarization (circle) and vertical (star) polarization states using the US standard atmospheric profile with sea surface wind speed being 5 m/s and sea surface temperature being 290 K.

Summary and Conclusions

- For non-opaque clouds, cloud parameters derived from Vis/IR window channels (e.g. effective size, cloud top) can significantly improve forward computations at IR sounding channels that are affected by clouds

- For microwave sounding channels, brightness temperatures in precipitating atmospheres are also affected by precipitation size and thus accurate forward simulations also require a good knowledge of particle size information

- From Cloudsat and AMSU collocated data, we found the biases of AMSU channels 1 to 4 over oceans are dependent on LWP. These biases may be related to Mie table used in CRTM for microwave simulations

- Accuracy for simulating the IR shortwave channels from 3 to 5 micron can be improved dramatically when NLTE and solar reflection at surfaces are included in CRTM calculations

- For conical scanning microwave imaging instruments, simulations of brightness temperatures must include the relative azimuthal angle

- For cross-track scanning microwave sounders, simulations of brightness temperatures require a full Stokes radiative transfer which is not handled in either CRTM or RTTOV